



1 **Effectiveness evaluation of temporary emission control action in 2016**
2 **winter in Shijiazhuang, China**

3
4 Baoshuang Liu^a, Yuan Cheng^a, Ming Zhou^a, Danni Liang^a, Qili Dai^a, Lu Wang^a, Wei Jin^b, Lingzhi
5 Zhang^b, Yibin Ren^b, Jingbo Zhou^b, Chunling Dai^b, Jiao Xu^a, Jiao Wang^a, Yinchang Feng^{a*}, and
6 Yufen Zhang^{a*}

7
8
9
10
11
12
13
14
15
16 ^a State Environmental Protection Key Laboratory of Urban Ambient Air Particulate Matter
17 Pollution Prevention and Control, College of Environmental Science and Engineering, Nankai
18 University, Tianjin, 300071, China
19 ^b Environmental Monitoring Station, Shijiazhuang, Hebei, 050023, China

* Tel./fax: +86 02285358792.

E-mail address: fengyc@nankai.edu.cn (Y. Feng) and zhafox@126.com (Y. Zhang)



Abstract.

To evaluate the environmental effectiveness of the control measures for atmospheric pollution in Shijiazhuang of China, a large-scale controlling experiment for emission sources of atmospheric pollutants (i.e., a temporary emission control action, TECA) was designed and implemented during November 1, 2016 to January 9, 2017. Under the unfavorably meteorological conditions, the mean concentrations of $\text{PM}_{2.5}$, PM_{10} , SO_2 , NO_2 , and chemical species (Si , Al , Ca^{2+} , Mg^{2+}) in $\text{PM}_{2.5}$ during the control action and heating period (CAHP) still decreased by 15 %, 26 %, 5 %, 19 %, 30.3 %, 4.5 %, 47.0 % and 45.2 %, respectively, compared to the no control action and heating period (NCAHP); indicating that the control measures of atmospheric pollution in Shijiazhuang were effective and was in a right direction. Overall, the effects of control measures in suburbs were better than those in urban area, especially for the control effects of particulate matters sources. The control effects for emission sources of carbon monoxide (CO) were not apparent during the TECA period, especially in suburbs, which is likely due to the increasing usage of domestic coal in suburbs along with the temperature decreasing.

The results of PMF analysis showed that crustal dust, secondary sources, vehicle emissions, coal combustion and industrial emissions were major $\text{PM}_{2.5}$ sources. Compared to the whole year, the contributions of coal combustion to $\text{PM}_{2.5}$ increased significantly during the CAHP and after control action (ACA); while the contribution proportions of crustal dust and vehicle emissions to $\text{PM}_{2.5}$ decreased apparently during the CAHP. The contribution concentrations and proportions of crustal dust and vehicle emissions to $\text{PM}_{2.5}$ during the CAHP also decreased significantly compared to ACA. The pollutant's emission sources during the CAHP were in effective control, especially for crustal dust and vehicles. While the necessary coal heating for cold winter and the unfavorably meteorological conditions had an offset effect on the control measures for emission sources to some extent. Meanwhile, our results also illustrated that the discharge of pollutants was still enormous even under such strict control measures.

The backward trajectory and potential source contribution function (PSCF) analysis in the light of atmospheric pollutants suggested that the potential sources-areas mainly concentrated in surrounding regions of Shijiazhuang, i.e., south of Hebei, north of Henan and Shanxi. The regional nature of the atmospheric pollution in Northern China Plain revealed that there is an urgent need for making cross-boundary control policy except for local control-measures given the high background



52 level of pollutants.

53 The TECA is an important practical exercise but it can't be advocated as the normalized control
54 measures for atmospheric pollution in China. The direct cause of atmospheric pollution in China is
55 the emission of pollutants exceeds the air environment's self-purification capacity, and the essential
56 reason is unreasonable and unhealthy pattern for economic development of China.

57

58 **Keywords:** Atmospheric pollutants; Effectiveness evaluation; Control action; PMF; PSCF

59



60 1 Introduction

61 As a consequence of rapid industrialization and urbanization, China has been suffering from
62 air quality degradation in recent years (Fu et al., 2014; Gao et al., 2015; Han et al., 2014; Hao et al.,
63 2017; Zhao et al., 2011). Frequently occurred severe haze is featured by long duration, extensive
64 coverage and sharply-increasing particulate concentration (Jiang and Xia, 2017; Tao et al., 2014;
65 Wang et al., 2016a; Zhang et al., 2015a). It has been suggested that severe haze pollution increase
66 the risk of respiratory and cardiovascular diseases (Chen et al., 2013; Gao et al., 2015; Pan et al.,
67 2014; Zhang et al., 2014a; Zhou et al., 2015). On the basis of previous statistics, there are four haze-
68 prone city clusters in China, including Beijing-Tianjin-Hebei region, Yangtze River Delta, Pearl
69 River Delta and Sichuan Basin (Bi et al., 2014; Chen et al., 2016a; Fu et al., 2014; Fu and Chen,
70 2017; Li et al., 2016b; Tao et al., 2013a; Wang et al., 2015b; Wu et al., 2008; Zhang et al., 2015b).
71 In recent years, the role of particulates in hazy events has been becoming more and more prominent.
72 The particulates can be discharged from varieties of sources or formed by physicochemical/aqueous-
73 oxidation reactions between gaseous precursors, which have significant negative effects on climate,
74 atmospheric visibility and public health (Chen et al., 2015; Fu and Chen, 2017; Lee et al., 2015;
75 Quinn and Bates, 2003; Shen et al., 2015; Tai et al., 2010; Zhang et al., 2010). The high observed
76 concentrations of fine particles and prolonged haze events have occurred frequently during autumn
77 and winter, and covered large regions in China. In some cases, the instantaneous mass concentration
78 of $\text{PM}_{2.5}$ had reached $1000 \mu\text{g}/\text{m}^3$ (Qin et al., 2016; Zhang et al., 2014b), which caused the extensive
79 concern from citizens and government agencies.

80 Confronted with severe air pollution and degradation of air quality, the government has carried
81 out a variety of control measures in recent years, including odd-and-even license plate rule
82 (<http://www.sjz.gov.cn/col/1274081553614/2016/11/17/1479391129628.html>), mandatory
83 installation of desulfurization, denitration and other pollution-controlling facilities in factories (Liu
84 et al., 2017a; Ma et al., 2015; Peng et al., 2017) and on-line monitoring system structure plan in
85 construction sites, etc. The atmospheric quality in China has been notably improved so far. From
86 2013 to 2016, the concentrations of atmospheric pollutants showed a decreased trend, and the annual
87 mean concentrations of $\text{PM}_{2.5}$, PM_{10} , SO_2 and NO_2 , in 2016 reached up to $50 \mu\text{g}/\text{m}^3$, $85 \mu\text{g}/\text{m}^3$, 21
88 $\mu\text{g}/\text{m}^3$ and $39 \mu\text{g}/\text{m}^3$, respectively, and significantly lower than those in 2013
89 (<http://www.zhb.gov.cn/hjzl/zghjzkgb/lnzghjzkgb/>). However, the concentrations of $\text{PM}_{2.5}$ and



90 PM_{10} in 2016 were still 1.4 and 1.2 times higher than the national ambient air quality standard
91 (NAAQS) (GB3095-2012 Grade II, $\text{PM}_{2.5}$: $35 \mu\text{g}/\text{m}^3$, PM_{10} : $70 \mu\text{g}/\text{m}^3$). Note that the concentrations
92 of $\text{PM}_{2.5}$ and PM_{10} during Beijing-Tianjin-Hebei region were up to $71 \mu\text{g}/\text{m}^3$ and $119 \mu\text{g}/\text{m}^3$ in 2016,
93 and 2.0 and 1.7 times higher than the NAAQS, respectively. Therefore, China still has a lot of work
94 to do to improve the national air quality.

95 Over the last decade, Chinese government has implemented stricter control-measures for
96 emission sources during multiple international events held in China than normal times (Chen et al.,
97 2016b; Guo et al., 2013; Liu et al., 2013; Sun et al., 2016; Wang et al., 2010; Wang et al., 2017). For
98 instance, the first attempt took place during the Beijing 2008 Olympic Games (Guo et al., 2013).
99 Drastic control actions were executed to cut down the emissions of atmospheric pollutants from
100 motor vehicles, industries and building construction activity (UNEP, 2009; Wang et al., 2009a; Wang
101 et al., 2010). UNEP (2009) suggested that the concentration of PM_{10} in Beijing was reduced by 20 %
102 due to the emission reduction measures. Liu et al. (2013) reported that the concentrations of SO_2 ,
103 NO_2 , PM_{10} and $\text{PM}_{2.5}$ were reduced by 66.8 %, 51.3 %, 21.5 % and 17.1 %, respectively, during the
104 2010 Asian Games in Guangzhou of China, and during which stricter control measures for emission
105 sources were implemented. Furthermore, further stricter controls for emission sources were
106 implemented in both Beijing and its surrounding regions during the 2014 Asia-Pacific Economic
107 Cooperation (APEC) summit and Parade. Compared to no-control during APEC and Parade, a
108 decreasing trend with 51.6~65.1 % and 34.2~64.7 % of $\text{PM}_{2.5}$ concentrations during the control
109 period was reported (Wang et al., 2017). Eventually, all the efforts led to a blue-sky days during the
110 APEC, which was acknowledged as “APEC Blue” (Wang et al., 2016b). As we can see that the air
111 quality can be improved in response to stricter emission controls in international events held in
112 China. However, once these stricter control-measures of emission sources were repealed, and the
113 air quality would be deteriorated subsequently
114 (http://www.mep.gov.cn/gkml/hbb/qt/201412/t20141218_293152.htm), indicating that the
115 prevention and control of air pollution in China still had a long way to go.

116 Shijiazhuang (38.03°N , 114.26°E), a hinterland city of Northern China Plain with a high
117 population density, is an important city in Beijing-Tianjin-Hebei region (Sun et al., 2013). The rapid
118 industry development has a great contribution to this city’s economic growth and degradation of air
119 quality at the same time (Du et al., 2010; Li et al., 2015; Yang et al., 2015, 2016a). Shijiazhuang has



120 been one of the cities with the most serious air pollution in the world
121 (<https://www.statista.com/chart/4887/the-20-worst-cities-worldwide-for-air-pollution/>), and
122 deteriorating air quality poses a great risk to public health (<http://www.who.int/ceh/risks/cehair/en/>),
123 as well as drags on the expansion of the economy. The government of Shijiazhuang has adopted a
124 variety of control measures (<http://www.sjzhb.gov.cn/>), however, it seems that the improvement in
125 air quality of Shijiazhuang is not go into effect so far, and the atmospheric pollution is still heavy.
126 In 2016, the annual concentrations of PM_{2.5} and PM₁₀ in Shijiazhuang reached up to 70 µg/m³ and
127 123 µg/m³, respectively, which were 2.0 and 1.8 times higher than the NAAQS (GB3095-2012
128 Grade II) (http://www.zhb.gov.cn/hjzl/tj/201706/t20170606_415527.shtml). Especially in the
129 heating period in winter, the degree of atmospheric pollution in Shijiazhuang was even more serious.
130 The effectiveness of control measures has been queried in recent years. Therefore, based on previous
131 examples of APEC, Parade and the Asian Games, etc., a large-scale controlling experiment for
132 atmospheric pollutants sources (i.e., TECA) was designed and implemented to investigate whether
133 control measures in Shijiazhuang are effective for the atmospheric pollution. The experiment was
134 carried out in Shijiazhuang during November 1 2016 to January 9 2017, during which more stringent
135 control measures of atmospheric pollution than usual were put into practice. Then, by combining of
136 the changes of atmospheric pollutants concentrations, emission source contributions and other
137 factors such as meteorological conditions, regional transmission, etc., the effectiveness of control
138 measures was evaluated before and after the control measures were taken.

139 2 Materials and Methods

140 2.1 Site description

141 Shijiazhuang city is located in the east of Taihang Mountain in north of China (Fig. 1), and the
142 urban area is 15848 km², with a population of more than 10 million in 2016. Shijiazhuang is a large
143 industrial city that is famous for raw materials, energy production and steel, power, and cement
144 industries. The number of vehicles is more than 2.0 million until 2016. Shijiazhuang has a typical
145 temperate and monsoonal climate with four clearly distinct seasons, with northeasterly,
146 southeasterly and northwesterly winds prevailed during the TECA period (Fig. S1). The mean wind
147 speed was 0.6 m/s, and the average temperature was 14.9 °C during the TECA period. The mean
148 relative humidity was up to 76.5 %, and the mean height of mixed layer was 509 m during the TECA
149 period. The meteorological conditions during the four stages of the TECA period in Shijiazhuang



were shown in Table 1.

The seven monitoring sites including Twenty-second Middle School (TSMS), High-tech Zone (HTZ), Great Hall of the People (GHP), Century Park (CP), Water Source Area in the Northwest (WSAN), University Area in the Southwest (UAS) and Staff Hospital (SH) are located in urban area of Shijiazhuang. While other seventeen sites including Fenglong Mountain (FLM), Gaoyi (GY), Gaocheng (GC), Xingtang (XT), Jinzhou (JZ), Jingxing Mining District (JXMD), Lingshou (LS), Luquan (LQ), Luancheng (LC), Pingshan (PS), Shenze (SZ), Wuji (WJ), Xinle (XL), Yuanshi (YS), Zanhuan (ZH), Zhaoxian (ZX) and Zhengding (ZD) are suited in suburbs of Shijiazhuang. The more details were shown in Table S1.

Fig. 1. Maps of the online monitoring stations and the filter membrane sampling sites in Shijiazhuang. The 24 online monitoring stations mainly include Twenty-second Middle School (TSMS), Fenglong Mountain (FLM), High-tech Zone (HTZ), Great Hall of the People (GHP), Century Park (CP), Water Source Area in the Northwest (WSAN), University Area in the Southwest (UAS), Staff Hospital (SH), Gaoyi (GY), Gaocheng (GC), Xingtang (XT), Jinzhou (JZ), Jingxing Mining District (JXMD), Lingshou (LS), Luquan (LQ), Luancheng (LC), Pingshan (PS), Shenze (SZ), Wuji (WJ), Xinle (XL), Yuanshi (YS), Zanhuan (ZH), Zhaoxian (ZX) and Zhengding (ZD). The filter membrane sampling sites are mainly located in TSMS, LQ and LC.

Table 1. The meteorological conditions during the four stages (NCANHP, NCAHP, CAHP and ACA) of the TECA period in Shijiazhuang.

2.2 Sampling and Analysis

2.2.1 Sampling

From November 1, 2016 to January 9, 2017, the concentrations of $PM_{2.5}$, PM_{10} , SO_2 , NO_2 , CO , O_3 and synchronous meteorological conditions (temperature, relative humidity, wind speed and wind direction) were monitored in the 24 monitoring sites belonged to national, provincial and city controlling points (Fig. 1). The more details about monitoring instruments were described in Table S2. The heights of mixed layer were measured with a lidar scanner (AGHJ-I-LIDAR (HPL)), which was set at an atmospheric gradient monitoring station in Shijiazhuang near CP site (Fig. 1), and more details were shown in supplemental material. The $PM_{2.5}$ filter membrane samples were collected in TSMS, LQ, and LC sites from November 24, 2015 to January 9, 2017. Three sampling sites were set on the rooftops of buildings at 12-15 meters above ground level. Meanwhile, the parallel samples and the field blanks were also collected at each site. More details about filter membrane sampling were shown in Table S3. Before sampling, the quartz filter membranes (47 mm



183 in diameter, Whatman, England) and polypropylene filter membranes (47 mm in diameter, Beijing
184 Synthetic Fiber Research Institute, China) were baked in the oven at 500 °C and 60 °C, respectively.
185 All the filter membranes after sampling were stored at 4 °C before subsequent gravimetric and
186 chemical analysis to improve the accuracy of experimental results.

187 2.2.2 Gravimetric and Chemical analysis

188 A 24-hour equilibrium process of PM_{2.5} filter membranes was performed at a condition of
189 constant temperature (20 ± 1 °C) and humidity (45-55 %) before gravimetric analysis. For the
190 gravimetric analysis, all the filter membranes were weighted twice on a microbalance with
191 resolution of 0.01 mg (Mettler Toledo, XS105DU) before and after sampling. An electrostatic
192 eliminating device was applied to ensure the accuracy of gravimetric results.

193 After the gravimetric analysis, the quartz filter membranes which carried atmospheric
194 particulates were used to analyze water-soluble ions by Ion chromatography (Thermo Fisher
195 Scientific, Dionex, ICS-5000+). One-eighth of the filter membrane was cut up and put into a 25 mL
196 glass tube with 20 mL ultrapure water. After 1-hour ultrasonic extraction and 3 minutes
197 centrifugalization, the supernatant was filtered with disposable filter head (0.22 µm) for subsequent
198 instrumental analysis. The ions analyzed included SO₄²⁻, NO₃⁻, Cl⁻, NH₄⁺, K⁺, Ca²⁺, Na⁺ and Mg²⁺,
199 and more details were shown in Figs. S2 and S3. Prior to the ions detection, standard solutions were
200 prepared and detected for over three times and low relative standard deviations (RSD) were obtained.
201 Analytical quantification was carried out by using calibration curves made from standard solutions
202 prepared.

203 Polypropylene filter membranes were used for elemental analysis by inductively coupled
204 plasma–mass spectrometry (ICP-MS, Agilent 7700x). Perchloric acid-nitric acid digestion method
205 was applied for the pretreatment of filter membranes. Aggregately, 10 elemental species (Al, Si, Ti,
206 Cr, Mn, Fe, Cu, Zn, As and Pb) were determined. The detection limits of all the elements were
207 shown in Table S4. For quality assurance and quality control (QA/QC), standard reference materials
208 were pre-treated and analyzed with the same procedure, with the recovered values for all the target
209 elements falling into the range or within 5 % of certified values.

210 The OC and EC were determined on a 0.558 cm² quartz filter membrane punch by Desert
211 Research Institute (DRI) Model 2001 Thermal/Optical Carbon Analyzer with IMPROVE A
212 thermal/optical reflectance (TOR) protocol. The quartz filter membrane was heated stepwise to



temperatures of 140 °C, 280 °C, 480 °C and 580 °C in a non-oxidizing helium (He) oven to analyse OC1, OC2, OC3 and OC4, respectively. Then, the oven was added to an oxidizing atmosphere of 2 % oxygen (O₂) and 98 % He, and the quartz filter membrane was gradually heated to 580 °C, 780 °C and 840 °C to analyse EC1, EC2 and EC3, respectively. The POC is defined as the carbon combusted after the initial introduction of oxygen and before the laser reflectance signal achieves its original value and the POC is specified as the fraction of OC. According to the IMPROVE A protocol, OC is defined as OC1+OC2+OC3+OC4+POC, and EC is defined as EC1+EC2+EC3-POC. For QA/QC, we carried out the measurement with the field blank filter membranes, standard sucrose solution and repeated analysis in the study. During each season, the field blanks were sampled and the particulate samples have been corrected by the average concentration of the blanks. For checking the precision of instrument, a replicate sample was analysed for every 10 samples, and the standard deviation $< \pm 5\%$ was accepted. The method detection limits (MDLs) of OC and EC are 0.45 and 0.06 $\mu\text{g}/\text{cm}^2$, respectively.

2.3 PMF model

PMF model can decompose a matrix of sample data (X) into two matrices: source profile (F) and source contribution (G), in terms of observations at the sampling sites (Paatero and Tapper, 1994). The principle of PMF model can be described by:

$$X_{ij} = \sum_{k=1}^p g_{ik} f_{kj} + e_{ij} \quad (1)$$

where X_{ij} represents concentration of the j^{th} species in the i^{th} sample, g_{ik} represents the contribution of the k^{th} source to the i^{th} sample, f_{kj} represents the source profile of j^{th} species from the k^{th} source, e_{ij} represents the residual for the j^{th} species in the i^{th} sample, and p represents the number of sources.

PMF can identify emission sources of PM_{2.5} without source profiles. Data below MDLs are retained for using in PMF model with the related uncertainty adjusted in terms of the characteristics that PMF model admits data to be signally weighed. To assess the stability of the solution, the object function Q can be allowed to review the distribution of each species, which is expressed by:

$$Q = \sum_{i=1}^n \sum_{j=1}^m \left[\frac{x_{ij} - \sum_{k=1}^p g_{ik} f_{kj}}{\mu_{ij}} \right]^2 \quad (2)$$

where μ_{ij} represents the uncertainty of j^{th} species in the i^{th} sample, which is applied to weight the observations that include the sampling errors, missing data, detection limits and outliers.

The purpose of PMF model was to minimize the function (Eq. (2)). Data below MDLs were



retained and their uncertainties were set to 5/6 of the MDLs. Missing values were replaced by the median concentration of a given species, with an uncertainty of four times the median (Brown et al., 2015). Values that were larger than the MDLs, the calculation of uncertainty was in terms of a user supplied fraction of the concentration and MDLs, and the error fraction was suggested as 10 % by Paatero (2000). Uncertainty was described by:

$$\text{Uncertainty} = \sqrt{(\text{Error Fraction} \times \text{concentration})^2 + (0.5 \times \text{MDL})^2} \quad (3)$$

In this study, EPA PMF 5.0 model was used to identify the PM_{2.5} sources in Shijiazhuang city. Based on the field investigation and change of Q values, and finally, five factors were chosen in PMF analysis. When five factors were chosen and input in PMF model, and the calculated Q value (5162) from PMF model was close to theoretical values (5045). The observed PM_{2.5} concentrations and calculated PM_{2.5} concentrations from PMF model showed high correlations ($r = 0.96$) (Fig. S4). S/N is the signal-to-noise ratio, which is used to address weak and bad variables when running PMF model (Paatero and Hopke, 2003). The signal vector is identified as S and the noise vector is identified as N. Next, S/N is defined as Eq. (4). Variables with $S/N \leq 0.2$ were removed from the analysis, while weak variables ($0.2 \leq S/N \leq 2.0$) were down-weighted (Ancelet et al., 2012). S/N of As, Ti and Cr were lower than 1.0 in this study, and these species were set as weak variables.

$$S/N = \sqrt{\sum s_i^2 / \sum n_i^2} \quad (4)$$

where i represents the chemical species in PM_{2.5}.

2.4 Backward trajectory and PSCF model

In this study, the 72-h backward trajectory arriving in Shijiazhuang (38.05° N, 55.2° E) was calculated at 1-h intervals during the CAHP by the Hybrid Single Particle Lagrangian Integrated Trajectory (HYSPLIT) model. The final global analysis data were produced from the National Center for Environmental Prediction's Global Data Assimilation System wind field reanalysis (<http://www.arl.noaa.gov/>). The model was run 4 times per day at starting times, i.e., 0:00, 06:00, 12:00, 18:00 LT; the starting height was set at 100 m above the ground. The PSCF model was used to identify the potential sources-areas in terms of the HYSPLIT analysis. The study region was divided into $i \times j$ small equal grid cells. The trajectory clustering and PSCF model were performed by using the GIS-based software TrajStat (Liu et al., 2017a; Wang et al., 2009b). The PSCF value was defined as:



$$\text{PSCF} = \frac{m_{ij}}{n_{ij}} \quad (5)$$

where i and j were the latitude and longitude indices, n_{ij} represented the number of endpoints that fell in the ij cell, and m_{ij} was the number of endpoints in the same cell that were related to the samples that were greater than the threshold criterion.

Based on the NAAQS (GB3095-2012 guideline value (24 h) of Grade II), the criterion values of $\text{PM}_{2.5}$, PM_{10} , NO_2 , CO were set to $75 \mu\text{g}/\text{m}^3$, $150 \mu\text{g}/\text{m}^3$, $80 \mu\text{g}/\text{m}^3$ and $4 \text{ mg}/\text{m}^3$, respectively. The criterion values of SO_2 and O_3 were set to $68 \mu\text{g}/\text{m}^3$ and $15 \mu\text{g}/\text{m}^3$ respectively, in terms of the average during the CAHP. When n_{ij} is smaller than three times the grid average number of trajectory endpoint (n_{ave}), a weighting function $W(n_{ij})$ was used to reduce uncertainty in cells (Dimitriou et al., 2015). The weighting function was defined by:

$$\text{WPSCF}_{ij} = \frac{m_{ij}}{n_{ij}} * W(n_{ij}) \quad (6)$$

$$W(n_{ij}) = \begin{cases} 1.00, 3n_{ave} < n_{ij} \\ 0.70, 1.5n_{ave} < n_{ij} \leq 3n_{ave} \\ 0.40, n_{ave} < n_{ij} \leq 1.5n_{ave} \\ 0.20, n_{ij} \leq n_{ave} \end{cases} \quad (7)$$

The studying field ranged from 33° N to 51° N , and 97° E to 121° E , and the region that was covered by the backward trajectories was divided into 432 grid cells of $1.0^\circ \times 1.0^\circ$. The total number of endpoints during the CAHP was 12672. Accordingly, there was an average of 5 trajectory endpoints in per cell ($n_{ave} = 5$).

2.5 Measures taken in the controlling experiment

The measures taken in the controlling experiment began on November 18, 2016 and ended on December 31, 2016 in Shijiazhuang (<http://www.sjz.gov.cn/col/1274081553614/2016/11/17/1479391129628.html>). The measures taken in the control action were mainly aimed at controlling emission sources of atmospheric pollutants in Shijiazhuang, which mainly included five aspects: (1) reduce the usage of coal, (2) decrease industrial production, (3) inhibition of dust emission, (4) driving restriction, and (5) prohibit open burning. The more details were described in supplemental material.

Actually, a total of 1543 enterprises were shut down in the whole city of Shijiazhuang during the control action period, including pharmaceutical, steel, cement, coking, casting, glass, ceramics, calcium and magnesium, sheet, sand and stone processing, stone processing and other industries.



298 The situation of specific closed-enterprises in different districts and counties is shown in Table S5.
299 In closed enterprises in Shijiazhuang, the number of mining and stone processing enterprises was
300 the largest, which was up to 733 and account for 48 % of all the closed enterprises. The numbers of
301 casting and building materials enterprises were up to 297 and 227, respectively, accounting for 19 %
302 and 15 % of the all, respectively. In addition, 64 enterprises related to pharmaceutical industry were
303 halted only for the VOC technology, and the 17 enterprises related to chemical industry must stop
304 production. The numbers of closed enterprises for cement and calcium/magnesium industry were
305 up to 49 and 40, respectively. The number of closed factories related to furniture and tanneries was
306 43, and the numbers of closed steel and coking enterprises were up to 4 and 7, respectively.

307 The average value of daily social-electricity consumption from November 18 to December 31,
308 2016 was 103,470,000 kW · h (Fig. S5), which declined 10 % compared to that of daily social-
309 electricity consumption from November 1 to 17, 2016, and declined 6 % compared to that of daily
310 social-electricity consumption during the same period in 2015. Restriction of motor vehicles based
311 on odd-and-even license plate rule in urban area of Shijiazhuang resulted in the decrease of the
312 average traffic-flow on arterial roads, which reduced about 30 % compared to before the control
313 action (Fig. S6). The dust emission can be reduced about 390 tons per day by a series of dust control-
314 measures. Compared to before the control action, the daily emissions of SO₂, NO_x, smoke dust and
315 VOCs reduced about 20 %, 33 %, 15 % and 7 %, respectively, during the control action period, on
316 the basis of the statistics on pollutants emission inventories.

317 **3 Results and discussion**

318 **3.1 Variations of atmospheric pollutants concentrations**

319 **3.1.1 Temporal trend**

320 The time series of atmospheric pollutants concentrations during the TECA period are shown in
321 Fig. 2. The average concentrations of PM_{2.5} and PM₁₀ during the TECA period in Shijiazhuang were
322 up to 181 µg/m³ and 295 µg/m³, respectively, which were 5.2 and 3.2 times than the Grade II limit
323 values in the NAAQS. The ratio of PM_{2.5}/PM₁₀ reached up to 0.62 during the TECA period,
324 indicating that the fine particulate dominated on the particulate pollution in Shijiazhuang. The mean
325 concentration of PM_{2.5} during the TECA period was significantly higher than those of winter in
326 Beijing (95.50 µg/m³), Tianjin (144.6 µg/m³), Hangzhou (127.9-144.9 µg/m³), Heze (123.6 µg/m³)
327 and Xinxiang (111 µg/m³) (Cheng et al., 2015; Gu et al., 2011; Liu et al., 2015; Liu et al., 2017a;



328 Feng et al., 2016), and lower than those of winter in Handan (240.6 $\mu\text{g}/\text{m}^3$) and Xian (266.8 $\mu\text{g}/\text{m}^3$)
329 (Meng et al., 2016; Zhang et al., 2011). Additionally, the NAAQS (GB3095-2012 Grade II) values
330 of SO_2 , NO_2 , CO and O_3 were 60 $\mu\text{g}/\text{m}^3$, 40 $\mu\text{g}/\text{m}^3$, 4 mg/m^3 and 160 $\mu\text{g}/\text{m}^3$, respectively. During
331 the TECA period, the average concentration of SO_2 (60 $\mu\text{g}/\text{m}^3$) could meet the NAAQS, and that of
332 NO_2 (81 $\mu\text{g}/\text{m}^3$) was far exceed the NAAQS; while those of CO (3.4 mg/m^3) and O_3 (15 $\mu\text{g}/\text{m}^3$)
333 were less than the NAAQS.

334 As well known, the date of coal-fired heating in Shijiazhuang began in November 15, 2016
335 (<http://www.sjz.gov.cn/col/1451896947837/2016/10/28/1477635691926.html>). Depending on the
336 changes of atmospheric pollution sources, the timeline of the TECA was divided into four stages:
337 stage 1: no control action and no heating period (NCANHP), ranging from November 1 to 14, 2016;
338 stage 2: no control action and heating period (NCAHP), ranging from November 15 to 17, 2016;
339 stage 3: control action and heating period (CAHP), ranging from November 18 to December 31,
340 2016; stage 4: after control action (ACA), ranging from January 1 to 9, 2017.

341 During the TECA period, the variations of atmospheric pollutants concentrations were mainly
342 affected by the heating for cold winter and the control measures of the control action except for the
343 meteorological conditions. Therefore, we defined the following equations to evaluate the effects of
344 the heating and control action, respectively, based on the atmospheric pollutants concentrations
345 during the different stages of TECA (i.e., NCANHP, NCAHP, CAHP and ACA).

346
$$P_{i\text{-heating}} = \frac{(C_{i\text{-NCAHP}} - C_{i\text{-NCANHP}}) \times 100}{C_{i\text{-NCANHP}}} \quad (8)$$

347
$$P_{i\text{-action}} = \frac{(C_{i\text{-NCAHP}} - C_{i\text{-CAHP}}) \times 100}{C_{i\text{-NCAHP}}} \quad (9)$$

348 where $P_{i\text{-heating}}$ represents the increasing percentage (%) of atmospheric pollutant concentration
349 because of the effects of heating for cold winter; $P_{i\text{-action}}$ represents the decreasing percentage (%)
350 of atmospheric pollutant concentration because of the control action; $C_{i\text{-NCANHP}}$ represents the
351 concentration ($\mu\text{g}/\text{m}^3$, CO: mg/m^3) of atmospheric pollutant during the no-control action and no-
352 heating period; $C_{i\text{-NCAHP}}$ represents the concentration ($\mu\text{g}/\text{m}^3$, CO: mg/m^3) of atmospheric pollutant
353 during the no-control action and heating period; $C_{i\text{-CAHP}}$ represents the concentration ($\mu\text{g}/\text{m}^3$, CO:
354 mg/m^3) of atmospheric pollutant during the control action and heating period.

355 During the NCANHP, the mean concentrations of $\text{PM}_{2.5}$ and PM_{10} were 156 $\mu\text{g}/\text{m}^3$ and 253
356 $\mu\text{g}/\text{m}^3$ in Shijiazhuang, respectively. With the beginning of heating, the mean concentrations of



PM_{2.5} and PM₁₀ increased 44 $\mu\text{g}/\text{m}^3$ and 64 $\mu\text{g}/\text{m}^3$ during the NCAHP, respectively, and the P_{PM_{2.5}-heating} and P_{PM₁₀-heating} values were up to 28 % and 25 % (Fig. 3 and Fig. 4). However, during the CAHP, the mean concentrations of PM_{2.5} and PM₁₀ were 185 $\mu\text{g}/\text{m}^3$ and 291 $\mu\text{g}/\text{m}^3$, respectively, which decreased by 15 % and 26 % compared to the NCAHP. And the P_{PM_{2.5}-action} and P_{PM₁₀-action} values are 8 % and 8 %, respectively. During the ACA, the concentrations of PM_{2.5} and PM₁₀ are 227 $\mu\text{g}/\text{m}^3$ and 383 $\mu\text{g}/\text{m}^3$, respectively, which increased significantly by 42 $\mu\text{g}/\text{m}^3$ and 92 $\mu\text{g}/\text{m}^3$ compared to the CAHP. The variations of SO₂ and NO₂ concentrations during different stages of TECA were similar to those of PM_{2.5} and PM₁₀ concentrations. The P_{SO₂-heating} and P_{NO₂-heating} values were 50 % and 33 %, respectively, and the P_{SO₂-action} and P_{NO₂-action} values were 5 % and 19 %. Well known that the NO₂ is mainly derived from the vehicle exhaust (Liu et al., 2017b). Therefore, the control effect of motor vehicles was remarkable during the CAHP in Shijiazhuang. Note that the mean concentration of CO in Shijiazhuang city varied from 2.2 mg/m^3 during the NCANHP to 5.5 mg/m^3 during the ACA period, which showed an increasing tendency (Fig. 3). Because CO was mainly produced from the uncompleted combustion of fossil fuels, so the usage of domestic coal might be increasing with the gradual decrease of temperature from the NCANHP (8.4 °C) to the ACA period (0.7 °C) (Table 1). Meanwhile, it can also be inferred that the control of domestic coal during the TECA period in Shijiazhuang city performed little efficiency. Because of the lack of emission inventories for domestic coal or small-boiler coal in Shijiazhuang, so that the control measures were less targeted. Additionally, the concentrations of O₃ during different stages of TECA were lower compared to other pollutants (Figs. 2 and 3). Overall, the control measures of emission sources in Shijiazhuang during the TECA period were go into effect, while the coal heating for cold winter and the unfavorable meteorological-conditions during the CAHP had an offset effect on the efforts of control measures for pollutant sources to some extent. The average wind speed during the CAHP (0.4 m/s on average) was lower than those during the other stages of the TECA period (0.5-0.7 m/s on average) (Table 1), and the wind directions were changeable (Fig. S1), which was in favor of the accumulation of atmospheric pollutants, and thus causing the concentrations of atmospheric pollutants to increase during the CAHP. Note that the heights of mixed layer showed an apparently decreasing tendency from the NCANHP (540 m on average) and the NCAHP (590 m on average) to the ACA (431 m on average), and the height of mixed layer during the CAHP was only 474 m on average (Table 1). The decrease in the height of mixed layer can cause the



concentrations of atmospheric pollutants near the ground to be compressed significantly and enhanced subsequently. In addition, during the CAHP, the multidirectional air-masses that were mainly originated from the Beijing-Tianjin-Hebei and its surrounding areas (e.g. Henan, Shandong and south of Hebei) displayed an overlap with each other in Shijiazhuang (Fig. S7), and further aggravate the level of air pollution in Shijiazhuang. Furthermore, the effects of control measures for domestic coal might be worse during the CAHP.

Fig. 2. The variations of atmospheric pollutants concentrations during the four stages (NCANHP, NCAHP, CAHP and ACA) of the TECA period in Shijiazhuang.

Fig. 3. The concentrations variations of $PM_{2.5}$, PM_{10} and gaseous pollutants during the four stages (NCANHP, NCAHP, CAHP and ACA) of the TECA period in Shijiazhuang.

Fig. 4. The $P_{i\text{-heating}}$ and $P_{i\text{-action}}$ of $PM_{2.5}$, PM_{10} and gaseous pollutants (SO_2 , NO_2 , CO and O_3) calculated by equation (8) and (9) in urban area and suburb in Shijiazhuang.

3.1.2 Spatial variation

The concentrations variations of $PM_{2.5}$, PM_{10} and related gaseous pollutants (SO_2 , NO_2 , CO and O_3) during four stages (NCANHP, NCAHP, CAHP and ACA) in urban area and suburb in Shijiazhuang are shown in Figs. 3 and 5. During the NCANHP, the average concentrations of $PM_{2.5}$ in urban area and suburb were $166 \mu g/m^3$ and $152 \mu g/m^3$, respectively. The concentrations of $PM_{2.5}$ in urban area and suburb increased significantly during the NCAHP (t-test, $p < 0.01$). The meanly increased concentration of $PM_{2.5}$ ($46 \mu g/m^3$) in urban area was higher than that of in suburb ($43 \mu g/m^3$), but the value of $P_{PM_{2.5}\text{-heating}}$ in suburb (29 %) was higher than that in urban area (27 %) (Fig. 4). Note that the mean concentration of $PM_{2.5}$ in urban area was up to $243 \mu g/m^3$ during the CAHP, which showed an increasing tendency, and the $P_{PM_{2.5}\text{-action}}$ value was -15 % (Fig. 4), likely due to the unfavorably meteorological conditions such as lower wind speed (0.4 m/s) and lower height of mixed layer (474 m), etc. (Table 1 and Fig. S7). Conversely, compared to the NCAHP, the concentrations of $PM_{2.5}$ in suburb (a mean of $161 \mu g/m^3$) decreased significantly during the CAHP (t-test, $p < 0.01$), and the $P_{PM_{2.5}\text{-action}}$ was up to 18 % (Fig. 4), indicating the control measures of $PM_{2.5}$ sources in suburb might be more effective than urban area. The tendency of SO_2 concentrations during different stages of TECA (except the ACA period) was similar to that of $PM_{2.5}$. The $P_{SO_2\text{-heating}}$ and $P_{SO_2\text{-action}}$ values in urban area were up to 58 % and -4 %, respectively, and were up to 47 % and 8 % in suburb during the TECA period (Fig. 4). However, the concentrations of SO_2 in urban



419 area and suburb decreased remarkably during the ACA compared to the CAHP (t-test, $p < 0.01$),
420 probably due to the effective control measures.

421 During the NCANHP, the average concentrations of PM_{10} in urban area and suburb were 280
422 and $242 \mu\text{g}/\text{m}^3$, respectively. Then, the meanly increased concentrations in urban area and suburb
423 were up to 65 and $64 \mu\text{g}/\text{m}^3$ during the NCAHP, which were comparable with each other.
424 Nevertheless, the mean $P_{PM_{10}\text{-heating}}$ value in suburb was higher (26 %) than that in urban area (23 %)
425 (Fig. 4). During the CAHP, the meanly decreased concentration of PM_{10} in urban area was $1 \mu\text{g}/\text{m}^3$,
426 and apparently lower than that of suburb ($36 \mu\text{g}/\text{m}^3$), as well as the mean $P_{PM_{10}\text{-action}}$ values in urban
427 area and suburb were 0.4 % and 12 %, respectively (Fig. 4). It can be seen that the control of PM_{10}
428 sources in suburb was more effective compared to urban area, in case of exclusion of unfavorably
429 meteorological conditions (Table 1 and Fig. S7), probably related to more than 700 enterprises
430 closed down which mainly carried out ore mining and stone processing in suburb (Tables S1 and
431 S5). The tendency of NO_2 concentrations in urban area and suburb was similar to that of PM_{10} during
432 different stages of TECA period. The mean $P_{\text{NO}_2\text{-heating}}$ values in urban area and suburb were up to
433 31 % and 34 %, respectively; while the mean $P_{\text{NO}_2\text{-action}}$ values in urban area and suburb were up to
434 17 % and 21 %, respectively. Note that the concentrations of CO in urban area and suburb showed
435 an increasing tendency from the NCANHP ($2.1\text{--}2.4 \text{ mg}/\text{m}^3$) to the ACA period ($5.5 \text{ mg}/\text{m}^3$) (Fig. 3).
436 The $P_{\text{CO-heating}}$ and $P_{\text{CO-action}}$ values in urban area were 22 % and -15 %, respectively, while those in
437 suburb were 32 % and -20 % during the TECA period. In addition, as shown in Fig. 5, the
438 concentrations of CO in the eastern and northern suburb in Shijiazhuang were significantly higher
439 than those of urban areas (t-test, $p < 0.01$). Note that the concentrations of O_3 in urban area and suburb
440 were lower during different stages of TECA (Fig. 5). Overall, during the TECA period, the effect of
441 control measures for atmospheric pollutants sources in suburb was better than in urban area,
442 especially for the effect of control measures for particulate matters sources. The effect of control
443 measures for CO was not notable during the TECA period, especially in suburb, likely due to the
444 increasing usage of domestic coal in suburb along with the temperature decreasing (Table 1).

445 ----

446 **Fig. 5.** The spatial variations of atmospheric pollutants ($PM_{2.5}$, PM_{10} , SO_2 , NO_2 , CO and O_3) during the four stages
447 (NCANHP, NCAHP, CAHP and ACA) of the TECA period in Shijiazhuang. The pictures were produced by ArcGIS
448 based kriging interpolation method.

449 ----



3.2 Variations of chemical species in PM_{2.5}

The average concentrations of chemical species in PM_{2.5} in Shijiazhuang during the whole sampling period are shown in Fig. 6. The annual mean concentrations of OC, SO₄²⁻, NO₃⁻ and NH₄⁺ in PM_{2.5} were 43.1 µg/m³, 39.0 µg/m³, 33.6 µg/m³ and 25.6 µg/m³, respectively, and their contributions to PM_{2.5} were up to 23.1 %, 20.0 %, 17.3 % and 12.3 %, respectively. The annual mean concentrations of EC and Cl⁻ were 11.7 µg/m³ and 7.7 µg/m³, respectively, which accounted for 5.9 % and 4.1 % of PM_{2.5}. Note that the annual mean concentrations of elements in PM_{2.5} were relatively lower, which varied from 0.03 to 2.6 µg/m³, accounting for 0.02–2.4 % of PM_{2.5}. Compared to other elements, the annual mean concentrations of Si (2.6 µg/m³) and Al (1.4 µg/m³) were relatively higher during the whole sampling period, which accounted for 2.4 % and 1.2 % of PM_{2.5}, respectively. In this study, the annual mean concentrations of OC, SO₄²⁻, NO₃⁻ and NH₄⁺ in Shijiazhuang were clearly higher than Beijing (Gao et al., 2016), Tianjin (Wu et al., 2015), Jinan (Gao et al., 2011), Shanghai (Wang et al., 2016c), Chengdu (Tao et al., 2013b), Xian (Wang et al., 2015a), Hangzhou (Liu et al., 2015) and Heze (Liu et al., 2017a).

The values of P_{i-heating} and P_{i-action} of different chemical species in PM_{2.5} were calculated by using the Eq. (8) and (9). The variations of chemical species in PM_{2.5} at four stages of the TECA and the values of P_{i-heating} and P_{i-action} in Shijiazhuang are shown in Figs. 7 and 8. Compared to the NCANHP, the concentrations of chemical species during the NCAHP showed a significantly increased tendency (t-test, $p < 0.01$), the concentrations of SO₄²⁻, Cl⁻, OC, EC, Si, Al, Ca²⁺ and Mg²⁺ increased by 7.9, 3.7, 6.7, 3.2, 1.6, 0.6, 0.4 and 0.1 µg/m³, respectively, and the P_{i-heating} values of these species were up to 30.0 %, 40.2 %, 14.6 %, 22.1 %, 78.8 %, 63.5 %, 47.4 % and 45.9 %, respectively, during the NCAHP. As these species (i.e., SO₄²⁻, Cl⁻, OC, EC, Si, Al, Ca²⁺ and Mg²⁺) were closely associated with coal combustion (Cao et al., 2011; Liu et al., 2015; Liu et al., 2016; Liu et al., 2017a, c), therefore, coal combustion for heating in winter probably had a great impact on increasing of these chemical species in PM_{2.5}. Furthermore, compared to the NCANHP, the concentrations of Cr, Cu, Fe, Mn, Ti, Zn and Pb increased by 0.02, 0.02, 0.34, 0.02, 0.02, 0.28 and 0.07 µg/m³, respectively, and the P_{i-heating} values of these species were 72.7 %, 33.1 %, 34.4 %, 21.0 %, 45.8 %, 48.3 % and 36.2 %, respectively, during the NCAHP. The Cr, Cu, Fe, Mn, Ti, Zn and Pb were closely related to industrial sources (Liu et al., 2015; Kabala and Singh, 2001; Morishita et al., 2011; Mansha et al., 2012; Yao et al., 2016), thus, the industrial emissions might have a higher



influence on $PM_{2.5}$ during the NCAHP than that during the NCANHP. Also, it might be closely associated with the unfavorably meteorological factors (Table 1 and Fig. S7).

Compared to the NCAHP, the concentrations of SO_4^{2-} , Cl^- , OC and EC during the CAHP increased by 16.8, 0.3, 19.8 and 14.6 $\mu g/m^3$, respectively, and the $P_{i-action}$ values of which were up to -48.8 %, -2.0 %, -37.3 % and -83.0 %, respectively, during the CAHP. As coal combustion was an important source of SO_4^{2-} , Cl^- , OC and EC (Cao et al., 2011; Liu et al., 2015; Liu et al., 2016; Liu et al., 2017a, c), so it can be inferred that the influence of coal combustion might increase apparently during the CAHP compared to the NCAHP, which was likely due to the increased usage of the coal for domestic heating with the reduction of temperature during winter (Table 1). As also Fig. 5 shown that the concentrations of CO during the CAHP were higher than those during the NCAHP, especially in rural areas. Furthermore, OC and EC were associated with the vehicle exhaust (Liu et al., 2016; Liu et al., 2017a), thus, the effect of motor vehicle management and control measures during the CAHP might be offset by the unfavorably meteorological conditions to some extent during the CAHP (Table 1 and Fig. S7). However, compared to the NCAHP, the concentrations of Si, Al, Ca^{2+} and Mg^{2+} during the CAHP decreased by 1.1, 0.1, 0.6 and 0.1 $\mu g/m^3$, respectively, and the $P_{i-action}$ values of which were up to 30.3 %, 4.5 %, 47.0 % and 45.2 %, respectively. As Si, Al, Ca^{2+} and Mg^{2+} were mainly originated from the crustal dust (Liu et al., 2016; Shen et al., 2010; Wang et al., 2015a; Yang et al., 2016b), therefore, the influence of crustal dust on $PM_{2.5}$ during the CAHP might decrease clearly compared to the NCAHP. That's closely related to the control measures of inhabitation of dust emission during the TECA period (as shown in section 2.5). In general, from the view of the variation of $PM_{2.5}$ speciation, there was no doubt that the TECA had a certain positive environmental effect on the improvement of air quality. However, the ambient pollutant concentration was impacted by not only the emission sources, but also the meteorological conditions, regional background level and distant transportation, it was understandable that the concentration of CO had a "rebound" effect during the CAHP as the height of mixing layer was only 474 m and a low wind speed of 0.4 m/s.

Fig. 6. The average concentrations and percentages of chemical species in $PM_{2.5}$ in Shijiazhuang during the whole sampling period: November 24, 2015 to January 9, 2017.

Fig. 7. The variations of chemical species in $PM_{2.5}$ during the four stages (NCANHP, NCAHP, CAHP and ACA) of the TECA period.



511 **Fig. 8.** The $P_{i\text{-heating}}$ and $P_{i\text{-action}}$ of chemical species in $\text{PM}_{2.5}$ during the TECA period in Shijiazhuang.

512 ----

513 3.3 Variations of $\text{PM}_{2.5}$ sources contributions

514 The filter membrane samples of $\text{PM}_{2.5}$ were collected in three sites (LQ, LC and TSMS) in
515 Shijiazhuang from November 24, 2015 to January 9, 2017, and source apportionment was carried
516 out by using EPA PMF 5.0, as well as five factors were identified during the period (Figs. 9 and 10).
517 The chemical profile of factor 1 was mainly represented by Si (72.3 %), Ca^{2+} (74.0 %), Mg^{2+} (43.9 %)
518 and Al (71.3 %), which were derived mainly from crustal dust (Liu et al., 2016; Shen et al., 2010;
519 Wang et al., 2015a). Thus, factor 1 was viewed as crustal dust. The contribution proportions of factor
520 1 to $\text{PM}_{2.5}$ decreased from 19.5 % ($38.5 \mu\text{g}/\text{m}^3$) during the whole year (WY) to 15.0 % ($40.3 \mu\text{g}/\text{m}^3$)
521 during the CAHP, and increased up to 16.3 % ($48.3 \mu\text{g}/\text{m}^3$) during the ACA. The main species of
522 factor 2 were SO_4^{2-} (53.9 %), NO_3^- (89.8 %) and NH_4^+ (75.0 %). Therefore, it was easily identified
523 as secondary sources (Liu et al., 2015, 2016, 2017a; Santacatalina et al., 2010; Srimuruganandam
524 and Nagendra, 2012). The contribution proportions of factor 2 to $\text{PM}_{2.5}$ ranged from 32.7 % (64.6
525 $\mu\text{g}/\text{m}^3$) during the WY to 31.6 % ($84.8 \mu\text{g}/\text{m}^3$), and decreased to 28.8 % ($85.2 \mu\text{g}/\text{m}^3$) during the
526 ACA. Factor 3 was represented by the relatively high loadings of OC (55.9 %), EC (70.9 %), Cu
527 (26.9 %) and Zn (26.5 %). Given that the OC and EC are generally predominant in the reported
528 source profile of vehicle exhaust (Liu et al., 2016, 2017a; Yao et al., 2016), and Zn is widely used
529 as an additive for lubricant in two-stroke engines, and Cu is closely associated with brake wear
530 (Begum et al., 2004; Canha et al., 2012; Lin et al., 2015; Liu et al., 2017a). Therefore, factor 3 was
531 identified as vehicle emissions. The contribution proportions of factor 3 to $\text{PM}_{2.5}$ decreased from
532 13.4 % ($26.4 \mu\text{g}/\text{m}^3$) during the WY to 10.6 % ($28.5 \mu\text{g}/\text{m}^3$) during the CAHP, and increased to 14.1 %
533 ($41.7 \mu\text{g}/\text{m}^3$) during the ACA. Factor 4 was characterized by the high contributions of Ca^{2+} (26.0 %),
534 Mg^{2+} (31.0 %), Si (13.3 %), As (84.9 %), Cl^- (38.6 %), OC (20.2 %) and SO_4^{2-} (26.7 %), and the
535 combination of these species in factor 4 inferred they were co-emission from coal combustion (Cao
536 et al., 2011; Liu et al., 2015, 2016, 2017a,c; Zhang et al., 2011). Therefore, factor 4 was identified
537 as coal combustion. The contribution proportions of factor 4 to $\text{PM}_{2.5}$ increased from 26.2 % (51.7
538 $\mu\text{g}/\text{m}^3$) during the WY to 31.7 % ($85.2 \mu\text{g}/\text{m}^3$) during the CAHP, and lightly increased to 32.6 %
539 ($96.3 \mu\text{g}/\text{m}^3$) during the ACA. Factor 5 was identified as industrial emissions, with high loadings of
540 Cr (66.7 %), Cu (63.7 %), Fe (83.2 %), Mn (51.3 %), Ti (70.0 %), Zn (69.2 %), Pb (42.1 %) and Cl



(41.0 %) (Almeida et al., 2015; Liu et al., 2015, 2016; Morishita et al., 2011; Mansha et al., 2012; Yao et al., 2016). The contribution proportions of factor 5 to $PM_{2.5}$ ranged from 5.1 % ($10.0 \mu g/m^3$) during the WY to 5.3 % ($14.2 \mu g/m^3$) during the CAHP, and decreased to 4.9 % ($14.4 \mu g/m^3$) during the ACA. Note that the contribution of industrial emissions to $PM_{2.5}$ was relatively lower than other sources (Fig. 10).

In general, crustal dust, secondary sources, vehicle emissions, coal combustion and industrial emissions were identified as $PM_{2.5}$ sources in Shijiazhuang. Compared to the WY, the contribution of coal combustion to $PM_{2.5}$ increased significantly during the CAHP and the ACA, which was closely associated with the coal heating for cold winter (Liu et al., 2016), and the unfavorably meteorological conditions (Table 1 and Fig. S7). Compared to the WY, the contribution proportions of crustal dust and vehicle emissions to $PM_{2.5}$ decreased apparently during the CAHP; and compared to the ACA, the contribution concentrations and proportions of which to $PM_{2.5}$ also decreased significantly during the CAHP. It indicated that the control effects of motor vehicles and crustal dust were remarkable during the CAHP, and the results were consistent with the above analysis. The contribution proportions of secondary sources to $PM_{2.5}$ during the CAHP and ACA showed little change compared to the WY. However, the contribution concentrations of secondary sources to $PM_{2.5}$ increased significantly during the CAHP and the ACA compared to the WY, likely due to frequent hazy events during the period, when there were significant secondary reactions (Han et al., 2014; Li et al., 2016a). In addition, it also illustrated that the discharge of atmospheric pollutants was still enormous even under such strict control measures. Note that the contribution concentrations of industrial emissions to $PM_{2.5}$ during the CAHP and ACA increased apparently compared to the WY, which probably was affected by adverse weather conditions during the period (Table 1 and Fig. S7).

Chen et al. (2016b) reported that the concentrations of particles during the 2014 Youth Olympic Games (YOG) period (August) were much lower than before-Games period (July) and after-Games period (September); and fugitive dusts, construction dusts and secondary sulfate aerosol decreased obviously in YOG, which means mitigation measures have played an effective role in reduction of particulate matter. Wang et al. (2017) found that the contributions of vehicles, industrial sources, fugitive dust, and other sources decreased 13.5-14.7 %, 10.7-11.2 %, 4.5-5.6 % and 1.7-2.7 %, respectively, during the Asia-Pacific Economic Cooperation (APEC) and China's Grand Military



571 Parade (CGMP), compared to the period before the control actions. Guo et al. (2013) found that
572 primary vehicle contributions were reduced by 30 % at the urban site and 24 % at the rural site,
573 compared with the non-controlled period before the Beijing 2008 Olympics. The reductions in coal
574 combustion contributions were 57 % at PKU site and 7 % at Yufa site. As we can see that these
575 control-actions of the strict measures taken for emission sources during the international events held
576 in China, including the TECA in Shijiazhuang, were all very important practical exercises and rarely
577 scientific experiments. However, it cannot be advocated as the normalized control measures for
578 atmospheric pollution in China. These strict measures taken during these periods are temporary, and
579 there is a normal recovery of all the emissions of sources after the operation. Once adverse weather
580 conditions occur, and the hazy events may continue to happen eventually. In short, the direct cause
581 of the severe atmospheric pollution in China is that the emission of pollutants beyond the air
582 environment's self-purification capacity, and the essential reason is unreasonable and unhealthy
583 pattern for economic development of China.

584 ----

585 **Fig. 9.** Source profiles obtained with the PMF for PM_{2.5}. Filled bars identify the species that mainly characterize
586 each factor profile.

587 **Fig. 10.** Source contributions of PM_{2.5} during different stages in Shijiazhuang. WY represents whole year: November
588 24, 2015 to January 9, 2017.

589 ----

590 3.4 Backward trajectory and PSCF analysis

591 The backward trajectory analysis was used to identify the transport pathways of the air mass
592 during the CAHP. In terms of the directions and travelled areas, these trajectories were divided into
593 the five groups (Fig. 11). Trajectory clusters 1, accounting for 31.3 % of the total, originated from
594 Shanxi province and passed over North of Hebei before arriving at Shijiazhuang. Trajectory cluster
595 1 reflected the features of small-scale, short-distance air mass transport (Fig. 11). The higher
596 concentrations of PM₁₀ (358 µg/m³), PM_{2.5} (237 µg/m³) and CO (3.9 µg/m³) might be due to the
597 variety of emission sources and the accumulation of pollutants from surrounding areas, since the
598 moving speed of air mass in cluster 1 was much lower than other trajectories (Fig. 11 and Table 2).
599 Trajectory cluster 2, 3 and 4 accounted for 58.0 % of the total trajectories, and began from the
600 northwest of China, passed through the Inner Mongolia and Shanxi, showing the features of large-
601 scale, long-distance air transports. The relative lower concentrations of PM₁₀ (189-290 µg/m³),



PM_{2.5} (119–181 $\mu\text{g}/\text{m}^3$), SO₂ (50–67 $\mu\text{g}/\text{m}^3$), NO₂ (58–78 $\mu\text{g}/\text{m}^3$) and CO (2.1–3.0 mg/m^3) were closely associated with high moving speeds of air mass (Fig. 11 and Table 2), and relatively less anthropogenic emission sources in the northwest of China. Trajectory cluster 5 was mainly originated from Ningxia province, passed over Shaanxi, Shanxi and Hebei before arriving at Shijiazhuang, accounting for 10.8 % of the total, showing the features of small-scale, short-distance air transport significantly elevated levels of PM₁₀ (451 $\mu\text{g}/\text{m}^3$), PM_{2.5} (303 $\mu\text{g}/\text{m}^3$), SO₂ (83 $\mu\text{g}/\text{m}^3$), NO₂ (104 $\mu\text{g}/\text{m}^3$) and CO (4.8 mg/m^3) with trajectory cluster 5 were associated with the sources and the accumulation of pollutants from surrounding areas. As well known that the Beijing-Tianjin-Hebei region was one of the severest polluted areas in China (Bi et al., 2014; Chen et al., 2013; Gu et al., 2011; Wang et al., 2014; Zhao et al., 2012), it might be an important reason why the concentrations of pollutants were higher with trajectory clusters 1 and 5 (Fig. 11 and Table 2).

In this study, PSCF model was used to analyze the potential sources-areas of atmospheric pollutants by combining backward trajectories and the concentrations of atmospheric pollutants in Shijiazhuang during the CAHP, and the results were shown in Fig. 12. The values of weighted potential source contribution function (WPSCF) of CO were higher in the north of Shaanxi, south of Shanxi and central and southern Inner Mongolia, which were mainly potential sources-areas of CO concentrations in Shijiazhuang (Fig. 12 (a)). The WPSCF values of NO₂ were higher in north of Henan and Shaanxi, Hebei, Shanxi, and central and southern Inner Mongolia, which were mainly potential sources-areas of NO₂ concentrations in Shijiazhuang (Fig. 12 (b)). The WPSCF values of O₃ and SO₂ were higher in the north of Henan and Shaanxi, Shanxi, and south of Hebei, which were distinguished as major potential sources-areas of O₃ and SO₂ concentrations in Shijiazhuang (Fig. 12 (c) and (d)). Moreover, the southwest of Shandong was also identified as mainly potential sources-areas of SO₂ concentrations in Shijiazhuang. As for PM_{2.5} and PM₁₀, the WPSCF values were higher in south of Hebei, and east of Shanxi, which were identified as mainly potential sources-areas of PM_{2.5} and PM₁₀ concentrations in Shijiazhuang (Fig. 12 (e) and (f)). Overall, the potential sources-areas of the atmospheric pollutants in Shijiazhuang mainly concentrated in the surrounding regions of Shijiazhuang, including south of Hebei, north of Henan and Shanxi. Previous studies also reported that Shanxi, Hebei and Henan provinces had serious air pollution problems (Feng et al., 2016; Kong et al., 2013; Meng et al., 2016; Zhu et al., 2011), revealing the regional nature of the atmospheric pollution in Northern Plain of China. Therefore, there is an urgent need for making



cross-boundary control policy except for local control-measures given the high background level of pollutants.

Fig. 11. Five clusters of the 72-h air mass backward trajectories during the CAHP. Red star represents Shijiazhuang city.

Fig. 12. Potential sources areas of atmospheric pollutants obtained from PSCF model during the CAHP. Red star represents Shijiazhuang city. The colors represent potential sources-areas influenced on the atmospheric pollutants, and the red color could be determined to be relatively important sources-areas while the blue color means unimportant potential sources-areas.

Table.2 The average concentrations of atmospheric pollutants in different clusters during the CAHP.

4 Conclusions

The control measures of atmospheric pollution in Shijiazhuang were effective and was in a right direction. Under unfavorably meteorological conditions, the mean concentrations of $\text{PM}_{2.5}$, PM_{10} , SO_2 , NO_2 , and chemical species (Si , Al , Ca^{2+} , Mg^{2+}) in $\text{PM}_{2.5}$ during the CAHP significantly decreased compared to the NCAHP. Overall, the effects of control measures in suburbs were better than in urban area, especially for the effects of control measures for particulate matters sources. The effects of control measures for CO emission sources were not apparent during the CAHP, especially in suburbs.

The pollutant's emission sources during the CAHP were in effective control, especially for crustal dust and vehicles. While the necessary coal heating for cold winter and the unfavorable meteorological conditions had an offset effect on the control measures for emission sources to some extent. The discharge of pollutants was still enormous even under such strict control measures.

The backward trajectory and PSCF analysis in the light of atmospheric pollutants suggested that the potential sources-areas mainly concentrated in surrounding regions of Shijiazhuang, i.e., south of Hebei, north of Henan and Shanxi. The regional nature of the atmospheric pollution in Northern China Plain revealed that there is an urgent need for making cross-boundary control policy except for local control-measures given the high background level of pollutants.

The TECA is an important practical exercise but it can't be advocated as the normalized control measures for atmospheric pollution in China. The direct cause of atmospheric pollution in China is the emission of pollutants exceeds the air environment's self-purification capacity, and the essential reason is unreasonable and unhealthy pattern for economic development of China.



664 Acknowledgments

665 This study was financially supported by the National Key Research and Development
666 Program of China (2016YFC0208500 & 2016YFC0208501) and Tianjin Science and Technology
667 Foundation (16YFZCSF00260) and the National Natural Science Foundation of China (21407081)
668 and the Fundamental Research Funds for the Central Universities. The authors thank Shijiazhuang
669 Environmental Protection Monitoring Station for their participating in the sampling campaign and
670 chemical analysis of samples.

671 Reference

- 672 Almeida, S.M., Lage, J., Fernández, B., Garcia, S., Reis, M.A., and Chaves, P.C.: Chemical
673 characterization of atmospheric particles and source apportionment in the vicinity of a
674 steelmaking industry, *Sci. Total Environ.*, 521–522, 411–420, 2015.
- 675 Ancelet, T., Davy, P.K., Mitchell, T., Trompette, W.J., Markwitz, A., and Weatherburn, D.C.:
676 Identification of particulate matter sources on an hourly time-scale in a wood burning
677 community, *Environ. Sci. Technol.*, 46, 4767–4774, 2012.
- 678 Begum, B.A., Kim, E., Biswas, S.K., and Hopke, P.K.: Investigation of sources of atmospheric
679 aerosol at urban and semi-urban areas in Bangladesh, *Atmos. Environ.*, 38, 3025–3038, 2004.
- 680 Bi, J.R., Huang, J.P., Hu, Z.Y., Holben, B.N., and Guo, Z.Q.: Investigating the aerosol optical and
681 radiative characteristics of heavy haze episodes in Beijing during January of 2013, *J. Geophys.*
682 *Res. Atmos.*, 119, 9884–9900, 2014.
- 683 Brown, S.G., Eberly, S., Paatero, P., and Norris, G.A.: Methods for estimating uncertainty in PMF
684 solutions: examples with ambient air and water quality data and guidance on reporting PMF
685 results, *Sci. Total Environ.*, 518–519, 626–635, 2015.
- 686 Canha, N., Freitas, M.C., Almeida-Silva, M., Almeida, S.M., Dung, H.M., Dionísio, I., Cardoso, J.,
687 Pio, C.A., Caseiro, A., Verburg, T.G., and Wolterbeek, H.T.: Burn wood influence on outdoor
688 air quality in a small village: Foros de Arrão, Portugal, *J. Radioanal. Nucl. Chem.*, 291, 83–88,
689 2012.
- 690 Cao, J.J., Chow, J.C., Tao, J., Lee, S.C., Watson, J.G., Ho, K.F., Wang, G.H., Zhu, C.S., and Han,
691 Y.M.: Stable carbon isotopes in aerosols from Chinese cities: influence of fossil fuels, *Atmos.*
692 *Environ.*, 45, 1359–1363, 2011.
- 693 Chen, X., Balasubramanian, R., Zhu, Q.Y., Behera, S.N., Bo, D.D., Huang, X., Xie, H.Y., and Cheng,



- 694 J.P.: Characteristics of atmospheric particulate mercury in size-fractionated particles during
695 haze days in Shanghai, Atmos. Environ., 131, 400–408, 2016a.
- 696 Chen, P.L., Wang, T.J., Lu, X.B., Yu, Y.Y., Kasoar, M., Xie, M., and Zhuang, B.L.: Source
697 apportionment of size-fractionated particles during the 2013 Asian Youth Games and the 2014
698 Youth Olympic Games in Nanjing, China, Sci. Total Environ., 579, 860, 2016b.
- 699 Chen, H. and Wang, H.: Haze Days in North China and the associated atmospheric circulations
700 based on daily visibility data from 1960 to 2012, J. Geophys. Res. Atmos., 120, 5895–5909,
701 2015.
- 702 Chen, R., Zhao, Z., and Kan, H.: Heavy smog and hospital visits in Beijing, China, Am. J. Respir.
703 Crit. Care Med., 188, 1170–1171, 2013.
- 704 Cheng, Y., He, K.B., Du, Z.Y., Zheng, M., Duan, F.K., and Ma, Y.L.: Humidity plays an important
705 role in the PM_{2.5} pollution in Beijing, Environ. Pollut., 197, 68–75, 2015.
- 706 Dimitriou, K., Remoundaki, E., Mantas, E., and Kassomenos, P.: Spatial distribution of source areas
707 of PM_{2.5} by Concentration Weighted Trajectory (CWT) model applied in PM_{2.5} concentration
708 and composition data, Atmos. Environ., 116, 138–145, 2015.
- 709 Du, W. P., Wang, Y. S., Song, T., Xin, J. Y., Cheng, Y. S., and Ji, D. S.: Characteristics of atmospheric
710 pollutants during the period of summer and autumn in Shijiazhuang, Environ. Sci., 31, 1409–
711 1416, 2010. (In Chinese)
- 712 Feng, J. L., Yu, H., Su, X. F., Liu, S. H., Li, Y., Pan, Y. P., and Sun, J. H.: Chemical composition and
713 source apportionment of PM_{2.5} during Chinese Spring Festival at Xinxiang, a heavily polluted
714 city in North China: fireworks and health risks, Atmos. Res., 182, 176–188, 2016.
- 715 Fu, G. Q., Xu, W. Y., Rong, R. F., Li, J. B., and Zhao, C. S.: The distribution and trends of fog and
716 haze in the North China Plain over the past 30 years, Atmos. Chem. Phys., 14, 11949–11958,
717 2014.
- 718 Fu, H. B., and Chen, J. M.: Formation, features and controlling strategies of severe haze-fog
719 pollutions in China, Sci. Total Environ., 578, 121–138, 2017.
- 720 Gao, J., Peng, X., Chen, G., Xu, J., Shi, G. L., Zhang, Y. C., and Feng, Y. C.: Insights into the
721 chemical characterization and sources of PM_{2.5} in Beijing at a 1-h time resolution, Sci. Total
722 Environ., 542, 162–171, 2016.
- 723 Gao, M., Guttikunda, S. K., Carmichael, G. R., Wang, Y., Liu, Z., Stanier, C. O., Saide, P. E., and



- 724 Yu, M.: Health impacts and economic losses assessment of the 2013 severe haze event in
725 Beijing area, *Sci. Total Environ.*, 511C, 553–561, 2015.
- 726 Gao, X. M., Yang, L. X., Cheng, S. H., Gao, R., Zhou, Y., Xue, L. K., Shou, Y. P., Wang, J., Wang,
727 X. F., Nie, W., Xu, P. J., and Wang, W. X.: Semi-continuous measurement of water-soluble ions
728 in PM_{2.5} in Jinan, China: Temporal variations and source apportionments, *Atmos. Environ.*, 45,
729 6048–6056, 2011.
- 730 Gu, J. X., Bai, Z. P., Li, A. X., Wu, L. P., Xie, Y. Y., Lei, W. F., Dong, H. Y., and Zhang, X.: Chemical
731 composition of PM_{2.5} during winter in Tianjin, China, *Particuology*, 9, 215–221, 2011.
- 732 Guo, S., Hu, M., Guo, Q., Zhang, X., Schauer, J. J., and Zhang, R.: Quantitative evaluation of
733 emission controls on primary and secondary organic aerosol sources during Beijing 2008
734 Olympics, *Atmos. Chem. Phys.*, 13, 8303–8314, 2013.
- 735 Han, S. Q., Wu, J. H., Zhang, Y. F., Cai, Z. Y., Feng, Y. C., Yao, Q., Li, X. J., Liu, Y. W., and Zhang,
736 M.: Characteristics and formation mechanism of a winter haze-fog episode in Tianjin, China,
737 *Atmos. Environ.*, 98, 323–330, 2014.
- 738 Hao, T. Y., Han, S. Q., Chen, S. C., Shan, X. L., Zai, Z. Y., Qiu, X. B., Yao, Q., Liu, J. L., Chen, J.,
739 and Meng, L. H.: The role of fog in haze episode in Tianjin, China: A case study for November
740 2015, *Atmos. Res.*, 194, 235–244, 2017.
- 741 Jiang, B. F., and Xia, D. H.: Role identification of NH₃ in atmospheric secondary new particle
742 formation in haze occurrence of China, *Atmos. Environ.*, 163, 107–117, 2017.
- 743 Kabala, C., and Singh, B.R.: Fractionation and mobility of copper, lead, and zinc in soil profiles in
744 the vicinity of a copper smelter, *J. Environ. Qual.*, 30, 485–492, 2001.
- 745 Kong, X. Z., He, W., Qin, N., He, Q. S., Yang, B., Ouyang, H. L., Wang, Q. M., and Xu, F. L.:
746 Comparison of transport pathways and potential sources of PM₁₀, in two cities around a large
747 Chinese lake using the modified trajectory analysis, *Atmos. Res.*, 122, 284–297, 2013.
- 748 Lee, H., Honda, Y., Hashizume, M., Guo, Y. L., Wu, C. F., Kan, H., Jung, K., Lim, Y. H., Yi, S., and
749 Kim, H.: Short-term exposure to fine and coarse particles and mortality: a multicity time-series
750 study in East Asia, *Environ. Pollut.*, 207, 43–51, 2015.
- 751 Li, J. J., Wang, G. H., Ren, Y. Q., Wang, J. Y., Wu, C., Han, Y. N., Zhang, L., Cheng, C. L., and
752 Meng, J. J.: Identification of chemical compositions and sources of atmospheric aerosols in
753 Xi'an, inland China during two types of haze events, *Sci. Total Environ.*, 566–567, 230–237,



- 2016a.
- Li, H. M., Wang, Q. G., Shao, M., Wang, J. H., Wang, C., Sun, Y. X., Qian, X., Wu, H. F., Yang, M., and Li, F. Y.: Fractionation of airborne particulate bound elements in haze-fog episode and associated health risks in a megacity of southeast China, *Environ. Pollut.*, 208, 655–662, 2016b.
- Li, M., Tang, G. Q., Huang, J., Liu, A. R., An, J. L., and Wang, Y. S.: Characteristics of winter atmospheric mixing layer height in Beijing-Tianjin-Hebei region and their relationship with the atmospheric pollution, *Environ. Sci.*, 36, 1935–1943, 2015. (In Chinese)
- Lin, Y.-C., Tsai, C.-J., Wu, Y.-C., Zhang, R., Chi, K.-H., Huang, Y.-T., Lin, S.-H., and Hsu, S.-C.: Characteristics of trace metals in traffic-derived particles in Hsuehshan Tunnel, Taiwan: size distribution, potential source, and finger printing metal ratio, *Atmos. Chem. Phys.*, 15, 4117–4130, 2015.
- Liu, B. S., Wu, J. H., Zhang, J. Y., Wang, L., Yang, J. M., Liang, D. N., Dai, Q. L., Bi, X. H., Feng, Y. C., Zhang, Y. F., and Zhang, Q. X.: Characterization and source apportionment of PM_{2.5} based on error estimation from EPA PMF 5.0 model at a medium city in China, *Environ. Pollut.*, 222, 10–22, 2017a.
- Liu, B. S., Yang, J. M., Yuan, J., Wang, J., Dai, Q. L., Li, T. K., Bi, X. H., Feng, Y. C., Xiao, Z. M., Zhang, Y. F., and Xu, H.: Source apportionment of atmospheric pollutants based on the online data by using PMF and ME2 models at a megacity, China, *Atmos. Res.*, 185, 22–31, 2017b.
- Liu, B. S., Li, T. K., Yang, J. M., Wu, J. H., Gao, J. X., Bi, X. H., Feng, Y. C., Zhang, Y. F., and Yang, H. H.: Source apportionment and a novel approach of estimating regional contributions to ambient PM_{2.5} in Haikou, China, *Environ. Pollut.*, 223, 334–345, 2017c.
- Liu, B. S., Song, N., Dai, Q. L., Mei, R. B., Sui, B. H., Bi, X. H., and Feng, Y. C.: Chemical composition and source apportionment of ambient PM_{2.5} during the non-heating period in Taian, China, *Atmos. Res.*, 170, 23–33, 2016.
- Liu, G., Li, J. H., Wu, D., and Xu, H.: Chemical composition and source apportionment of the ambient PM_{2.5} in Hangzhou, China, *Particuology*, 18, 135–143, 2015.
- Liu, H., Wang, X. M., Zhang, J. P., He, K. B., Wu, Y., and Xu, J. Y.: Emission controls and changes in air quality in Guangzhou during the Asian Games, *Atmos. Environ.*, 76, 81–93, 2013.
- Mansha, M., Ghauri, B., Rahman, S., and Amman, A.: Characterization and source apportionment of ambient air particulate matter (PM_{2.5}) in Karachi, *Sci. Total Environ.*, 425, 176–183, 2012.



- 784 Ma, Z.Z., Li, Z., Jiang, J.K., Ye, Z.X., Deng, J.G., and Duan, L.: Characteristics of water-soluble
785 inorganic ions in PM_{2.5} emitted from coal fired power plants, Environ. Sci., 36, 2361–2366,
786 2015. (In Chinese)
- 787 Meng, C. C., Wang, L. T., Zhang, F. F., Wei, Z., Ma, S. M., Ma, X., and Yang, J.: Characteristics of
788 concentrations and water-soluble inorganic ions in PM_{2.5} in Handan City, Hebei province, China,
789 Atmos. Res., 171, 133–146, 2016.
- 790 Morishita, M., Gerald, J., Keeler, G.J., Kamal, A.S., Wagner, J.G., Harkema, J.R., and Rohr, A.C.:
791 Source identification of ambient PM_{2.5} for inhalation exposure studies in Steubenville, Ohio
792 using highly time-resolved measurements, Atmos. Environ., 45, 7688–7697, 2011.
- 793 Paatero, P.: User's Guide for Positive Matrix Factorization Programs PMF2 and PMF3, Part 1:
794 Tutorial. University of Helsinki, Finland (February), 2000.
- 795 Paatero, P., and Hopke, P.K.: Discarding or down-weighting high-noise variables in factor analytic
796 models, Anal. Chim. Acta, 490, 277–289, 2003.
- 797 Paatero, P., and Tapper, U.: Positive matrix factorization: a non-negative factor model with optimal
798 utilization of error estimates of data values, Environ. Metrics., 5, 111–126, 1994.
- 799 Pan, Q., Yu, Y., Tang, Z., Xi, M., and Zang, G.: Haze, a hotbed of respiratory-associated infectious
800 diseases, and a new challenge for disease control and prevention in China, Am. J. Infect.
801 Control, 42, 688, 2014.
- 802 Peng, W., Yang, J. N., Wagner, F., and Mauzerall, D. L.: Substantial air quality and climate co-
803 benefits achievable now with sectoral mitigation strategies in China, Sci. Total Environ., 598,
804 1076–1084, 2017.
- 805 Qin, K., Wu, L. X., Wong, M. S., Letu, H., Hu, M. Y., Lang, H. M., Sheng, S. J., Teng, J. Y., Xiao,
806 X., and Yuan, L. M.: Trans-boundary aerosol transport during a winter haze episode in China
807 revealed by ground-based Lidar and CALIPSO satellite, Atmos. Environ., 141, 20–29, 2016.
- 808 Quinn, P. K., and Bates, T. S.: North American, Asian, and Indian haze: similar regional impacts on
809 climate? Geophys. Res. Lett., 30, 193–228, 2003.
- 810 Santacatalina, M., Reche, C., Minguillón, M. C., Escrig, A., Sanfelix, V., Carratalá, A., Nicolás, J.
811 F., Yubero, E., Crespo, J., Alastuey, A., Monfort, E., Miró, J. V., and Querol, X.: Impact of
812 fugitive emissions in ambient PM levels and composition: A case study in Southeast Spain, Sci.
813 Total Environ., 408, 4999–5009, 2010.



- 814 Shafer, M. M., Toner, B. M., Overdier, J. T., Schauer, J. J., Fakra, S. C., Hu, S., Herner, J. D., and
815 Ayala, A.: Chemical speciation of vanadium in particulate matter emitted from diesel vehicles
816 and urban atmospheric aerosols, *Environ. Sci. Technol.*, 46, 189–195, 2012.
- 817 Shen, Z. X., Cao, J., Arimoto, R., Han, Y. M., Zhu, C. S., Tian, J., and Liu, S. X.: Chemical
818 characteristics of fine particles (PM₁) from Xi'an, China, *Aerosol Sci. Technol.*, 44, 461–472,
819 2010.
- 820 Shen, X. J., Sun, J. Y., Zhang, X. Y., Zhang, Y. M., Zhang, L., Che, H. C., Ma, Q. L., Yu, X. M., Yue,
821 Y., and Zhang, Y. W.: Characterization of submicron aerosols and effect on visibility during a
822 severe haze-fog episode in Yangtze River Delta, China, *Atmos. Environ.*, 120, 307–316, 2015.
- 823 Srimuruganandam, B., and Nagendra, S. M. S.: Application of positive matrix factorization in
824 characterization of PM₁₀ and PM_{2.5} emission sources at urban roadside, *Chemosphere*, 88, 120–
825 130, 2012.
- 826 Sun, X., Yin, Y., Sun, Y. W., Sun, Y., Liu, W., and Han, Y.: Seasonal and vertical variations in aerosol
827 distribution over Shijiazhuang, China, *Atmos. Environ.*, 81, 245–252, 2013.
- 828 Sun, Y. L., Wang, Z. F., Wild, O., Xu, W. Q., Chen, C., Fu, P. Q., Du, W., Zhou, L. B., Zhang, Q.,
829 Han, T. T., Wang, Q. Q., Pan, X. L., Zheng, H. T., Li, J., Guo, X. F., Liu, J. G., and Worsnop,
830 D. R.: “APEC Blue”: Secondary Aerosol Reductions from Emission Controls in Beijing. *Sci.*
831 *Rep.*, 6, 20668, 2016.
- 832 Tai, A. P. K., Mickley, L. J., and Jacob, D. J.: Correlations between fine particulate matter (PM_{2.5})
833 and meteorological variables in the United States: implications for the sensitivity of PM_{2.5} to
834 climate change, *Atmos. Environ.*, 44, 3976–3984, 2010.
- 835 Tao, J., Zhang, L., Engling, G., Zhang, R., Yang, Y., Cao, J. J., Zhu, C. S., Wang, Q. Y., and Luo, L.:
836 Chemical composition of PM_{2.5} in an urban environment in Chengdu, China: importance of
837 springtime dust storms and biomass burning, *Atmos. Res.*, 122, 270–283, 2013a.
- 838 Tao, J., Cheng, T. T., Zhang, R. J., Cao, J. J., Zhu, L. H., Wang, Q. Y., Luo, L., and Zhang, L. M.:
839 Chemical Composition of PM_{2.5} at an Urban Site of Chengdu in Southwestern China, *Adv.*
840 *Atmos. Sci.*, 30, 1070–1084, 2013b.
- 841 Tao, M., Chen, L., Xiong, X., Zhang, M., Ma, P., Tao, J., and Wang, Z.: Formation process of the
842 widespread extreme haze pollution over northern China in January 2013: Implications for
843 regional air quality and climate, *Atmos. Environ.*, 98, 417–425, 2014.



- 844 UNEP, United Nations Environmental Programme: Independent Environmental Assessment Beijing
845 2008 Olympic Games, Nairobi, Kenya, 2009, online available at: http://www.unep.org/publications/UNEP-eBooks/BeijingReport_ebook.pdf, last access: March 2010.
- 846
847 Wang, G., Cheng, S. Y., Wei, W., Yang, X. W., Wang, X. Q. Jia, J., Lang, J. L., and Lv, Z.:
848 Characteristics and emission-reduction measures evaluation of PM_{2.5} during the two major
849 events: APEC and Parade, Sci. Total Environ., 595, 81–92, 2017.
- 850 Wang, G., Zhang, R., Gomez, M. E., Yang, L., Levy Zamora, M., Hu, M., Lin, Y., Peng, J., Guo, S.,
851 Meng, J., Li, J., Cheng, C., Hu, T., Ren, Y., Wang, Y., Gao, J., Cao, J., An, Z., Zhou, W., Li, G.,
852 Wang, J., Tian, P., Marrero-Ortiz, W., Secrest, J., Du, Z., Zheng, J., Shang, D., Zeng, L., Shao,
853 M., Wang, W., Huang, Y., Wang, Y., Zhu, Y., Li, Y., Hu, J., Pan, B., Cai, L., Cheng, Y., Ji, Y.,
854 Zhang, F., Rosenfeld, D., Liss, P. S., Duce, R. A., Kolb, C. E., and Molina, M. J.: Persistent
855 sulfate formation from London Fog to Chinese haze, Proc. Natl. Acad. Sci. U. S. A., 113,
856 13630–13635, 2016a.
- 857 Wang, H. B., Zhao, L. J., Xie, Y. J., and Hu, Q. M.: “APEC blue”—The effects and implications of
858 joint pollution prevention and control program, Sci. Total Environ., 553, 429–438, 2016b.
- 859 Wang, H. L., Qiao, L. P., Lou, S. R., Zhou, M., Ding, A. J., Huang, H. Y., Chen, J. M., Wang, Q.,
860 Tao, S. K., Chen, C. H., Li, L., and Huang, C.: Chemical composition of PM_{2.5} and
861 meteorological impact among three years in urban Shanghai, China, Journal of Cleaner
862 Production, 112, 1302–1311, 2016c.
- 863 Wang, P., Cao, J. J., Shen, Z. X., Han, Y. M., Lee, S. C., Huang, Y., Zhu, C. S., Wang, Q. Y., Xu, H.
864 M., and Huang, R. J.: Spatial and seasonal variations of PM_{2.5} mass and species during 2010
865 in Xi'an, China, Sci. Total Environ., 508, 477–487, 2015a.
- 866 Wang, Q. Z., Zhuang, G. S., Huang, K., Liu, T. N., Deng, C. R., Xu, J., Lin, Y. F., Guo, Z. G., Chen, Y.,
867 Fu, Q. Y., and Fu, J. S.: Probing the severe haze pollution in three typical regions of China:
868 Characteristics, sources and regional impacts, Atmos. Environ., 120, 76–88, 2015b.
- 869 Wang, L. T., Wei, Z., Yang, J., Zhang, Y., Zhang, F. F., Su, J., Meng, C. C., and Zhang, Q.: The 2013
870 severe haze over southern Hebei, China: model evaluation, source apportionment, and policy
871 implications, Atmos. Chem. Phys., 14, 3151–3173, 2014.
- 872 Wang, T., Nie, W., Gao, J., Xue, L. K., Gao, X. M., Wang, X. F., Qiu, J., Poon, C. N., Meinardi, S.,
873 Blake, D., Wang, S. L., Ding, A. J., Chai, F. H., Zhang, Q. Z., and Wang, W. X.: Air quality



- 874 during the 2008 Beijing Olympics: secondary pollutants and regional impact, Atmos. Chem.
875 Phys., 10, 7603–7615, 2010.
- 876 Wang, M., Zhu, T., Zheng, J., Zhang, R. Y., Zhang, S. Q., Xie, X. X., Han, Y. Q., and Li, Y.: Use of
877 a mobile laboratory to evaluate changes in on-road air pollutants during the Beijing 2008
878 Summer Olympics, Atmos. Chem. Phys., 9, 8247–8263, 2009a.
- 879 Wang, Y. Q., Zhang, X. Y., and Draxler, R.: TrajStat: GIS-based software that uses various trajectory
880 statistical analysis methods to identify potential sources from long-term air pollution
881 measurement data, Environ. Modell. Softw., 24, 938–939, 2009b.
- 882 Wu, H., Zhang, Y. F., Han, S. Q., Wu, J. H., Bi, X. H., Shi, G. L., Wang, J., Yao, Q., Cai, Z. Y., Liu,
883 J. L., and Feng, Y. C.: Vertical characteristics of PM_{2.5} during the heating season in Tianjin,
884 China, Sci. Total Environ., 523, 152–160, 2015.
- 885 Wu, D., Liao, G. L., Deng, X. J., Bi, X. Y., Tan, H. B., Li, F., Jiang, C. L., Xia, D., and Fan, S. J.:
886 Transport condition of surface layer under haze weather over the Pearl River Delta, Acta. Meteor.
887 Sin., 68, 680–688, 2008. (In Chinese).
- 888 Yang, L. L., Feng, Y., Jin, W., Li, Y. Q., Zhou, J. B., Jiang, J. B., and Li, Z. G.: Pollution
889 characteristic of water soluble inorganic ion in atmospheric particles in Shijiazhuang, Adm.
890 Tech. Environ., Monit., 26, 17–21, 2016a. (In Chinese).
- 891 Yang, H. N., Chen, J., Wen, J. J., Tian, H. Z., and Liu, X. G.: Composition and sources of PM_{2.5}
892 around the heating periods of 2013 and 2014 in Beijing: Implications for efficient mitigation
893 measures, Atmos. Environ., 124, 378–386, 2016b.
- 894 Yang, Y., Liu, X. G., Qu, Y., Wang, J. L., An, J. L., Zhang, Y. H. G., and Zhang, F.: Formation
895 mechanism of continuous extreme haze episodes in the megacity Beijing, China, in January
896 2013, Atmos. Res., 155, 192–203, 2015.
- 897 Yao, L., Yang, L. X., Yuan, Q., Yan, C., Dong, C., Meng, C. P., Sui, X., Yang, F., Lu, Y. L., and
898 Wang, W. X.: Sources apportionment of PM_{2.5} in a background site in the North China Plain,
899 Sci. Total Environ., 541, 590–598, 2016.
- 900 Zhang, X. Y., Wang, L., Wang, W. H., Cao, D. J., and Ye, D. X.: Long-term trend and spatiotemporal
901 variations of haze over China by satellite observations from 1979 to 2013, Atmos. Environ.,
902 119, 362–373, 2015a.
- 903 Zhang, L., Wang, T., Lv, M. Y., and Zhang, Q.: On the severe haze in Beijing during January 2013:



- 904 unraveling the effects of meteorological anomalies with WRF-Chem, Atmos. Environ., 104,
905 11–21, 2015b.
- 906 Zhang, Z. L., Wang, J., Chen, L. H., Chen, X. Y., Sun, G. Y., Zhong, N. S., Kan, H. D., and Lu, W.
907 J.: Impact of haze and air pollution-related hazards on hospital admissions in Guangzhou,
908 China, Environ. Sci. Pollut. Res. Int., 21, 4236–4244, 2014a.
- 909 Zhang, J. K., Sun, Y., Liu, Z. R., Ji, D. S., Hu, B., Liu, Q., and Wang, Y. S.: Characterization of
910 submicron aerosols during a month of serious pollution in Beijing, 2013, Atmos. Chem. Phys.,
911 14, 2887–2903, 2014b.
- 912 Zhang, T., Cao, J. J., Tie, X. X., Shen, Z. X., Liu, S. X., Ding, H., Han, Y. M., Wang, G. H., Ho, K.
913 F., Qiang, J., and Li, W. T.: Water-soluble ions in atmospheric aerosols measured in Xi'an,
914 China: seasonal variations and sources, Atmos. Res., 102, 110–119, 2011.
- 915 Zhang, Q. H., Zhang, J. P., and Xue, H. W.: The challenge of improving visibility in Beijing, Atmos.
916 Chem. Phys., 10, 7821–7827, 2010.
- 917 Zhao, B., Wang, P., Ma, J. Z., Zhu, S., Pozzer, A., and Li, W.: A high-resolution emission inventory
918 of primary pollutants for the Huabei region, China, Atmos. Chem. Phys., 12, 481–501, 2012.
- 919 Zhao, P. S., Zhang, X. L., and Xu, X. F.: Long-term visibility trends and characteristics in the region
920 of Beijing, Tianjin, and Hebei, China, Atmos. Res., 101, 711–718, 2011.
- 921 Zhou, M. G., He, G. J., Fan, M. Y., Wang, Z. X., Liu, Y., Ma, J., Ma, Z. W., Liu, J. M., Liu, Y. N.,
922 and Wang, L. D.: Smog episodes, fine particulate pollution and mortality in China, Environ.
923 Res., 136, 396–404, 2015.
- 924 Zhu, L., Huang, X., Shi, H., Cai, X. H., and Song, Y.: Transport pathways and potential sources of
925 PM₁₀ in Beijing, Atmos. Environ., 45, 594–604, 2011.

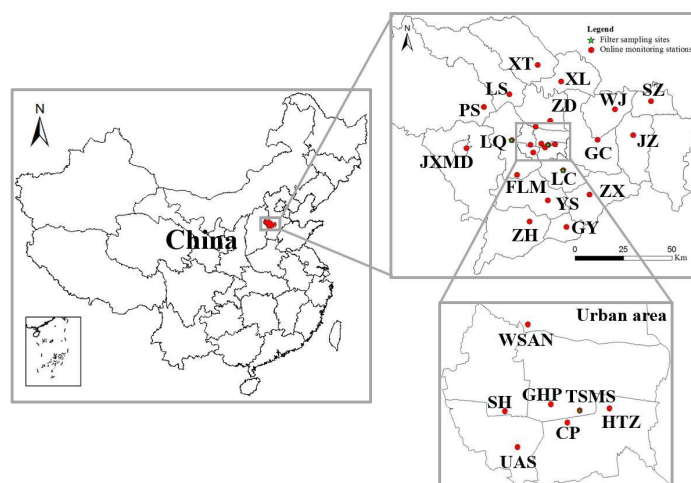


Fig. 1. Maps of the online monitoring stations and the filter membrane sampling sites in Shijiazhuang. The 24 online monitoring stations mainly include Twenty-second Middle School (TSMS), Fenglong Mountain (FLM), High-tech Zone (HTZ), Great Hall of the People (GHP), Century Park (CP), Water Source Area in the Northwest (WSAN), University Area in the Southwest (UAS), Staff Hospital (SH), Gaoyi (GY), Gaocheng (GC), Xingtang (XT), Jinzhou (JZ), Jingxing Mining District (JXMD), Lingshou (LS), Luquan (LQ), Luancheng (LC), Pingshan (PS), Shenze (SZ), Wuji (WJ), Xinle (XL), Yuanshi (YS), Zhanhuang (ZH), Zhaoxian (ZX) and Zhengding (ZD). The filter membrane sampling sites are mainly located in TSMS, LQ and LC.

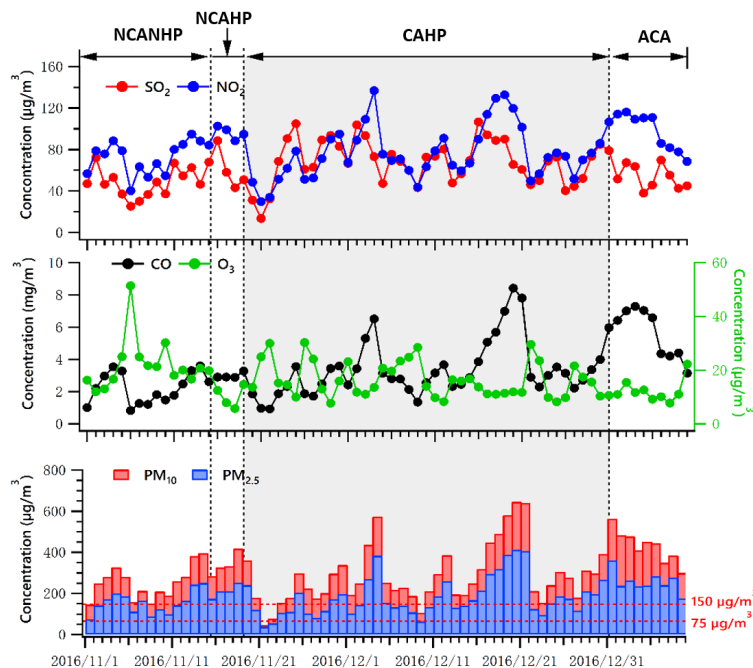


Fig. 2. The variations of atmospheric pollutants concentrations during the four stages (NCANHP, NCAHP, CAHP and ACA) of the TECA period in Shijiazhuang.

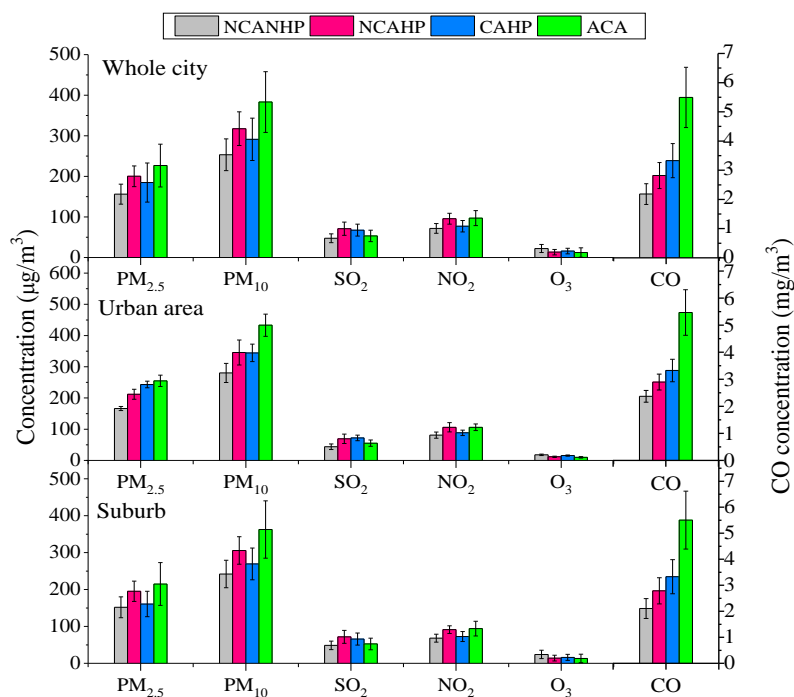


Fig. 3. The concentrations variations of PM_{2.5}, PM₁₀ and gaseous pollutants during the four stages (NCANHP, NCAHP, CAHP and ACA) of the TECA period in Shijiazhuang.

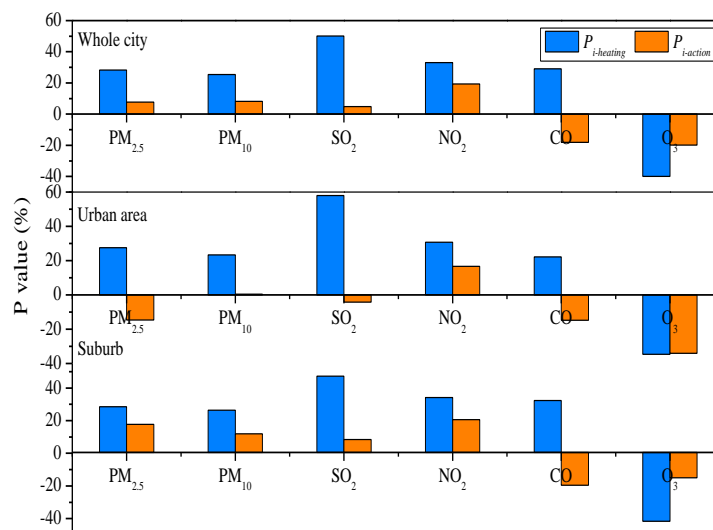


Fig. 4. The P_{heating} and P_{action} of PM_{2.5}, PM₁₀ and gaseous pollutants (SO₂, NO₂, CO and O₃) calculated by equation (8) and (9) in urban area and suburb in Shijiazhuang.

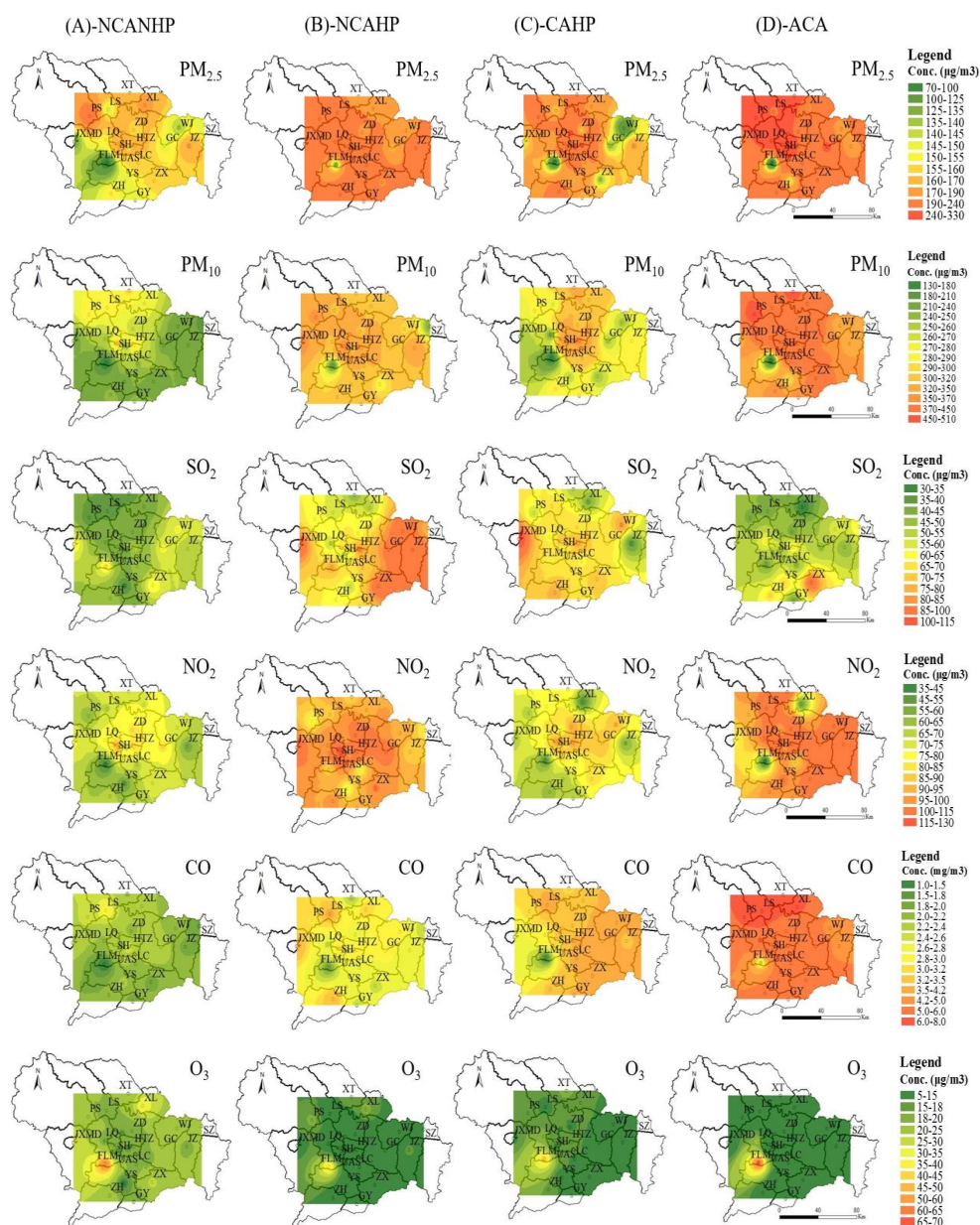


Fig. 5. The spatial variations of atmospheric pollutants (PM_{2.5}, PM₁₀, SO₂, NO₂, CO and O₃) during the four stages (NCANHP, NCAHP, CAHP and ACA) of the TECA period in Shijiazhuang. The pictures were produced by ArcGIS based kriging interpolation method.

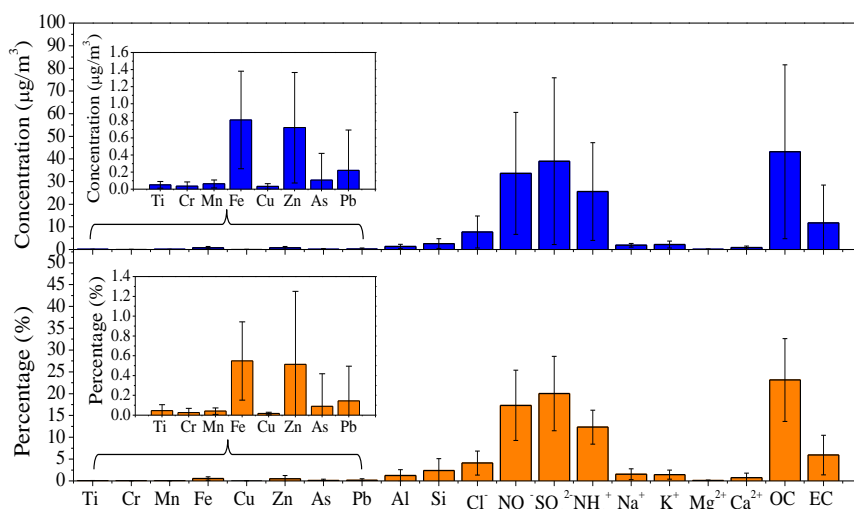


Fig. 6. The average concentrations and percentages of chemical species in $\text{PM}_{2.5}$ in Shijiazhuang during the whole sampling period: November 24, 2015 to January 9, 2017.

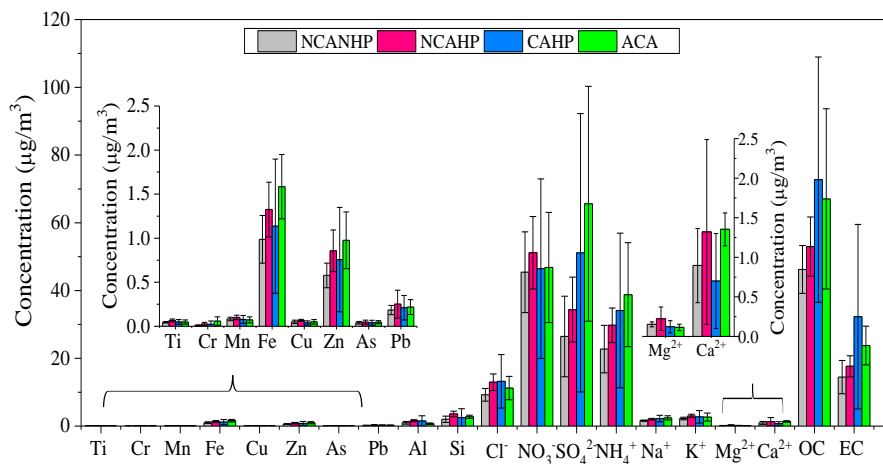


Fig. 7. The variations of chemical species in $\text{PM}_{2.5}$ during the four stages (NCANHP, NCAHP, CAHP and ACA) of the TECA period.

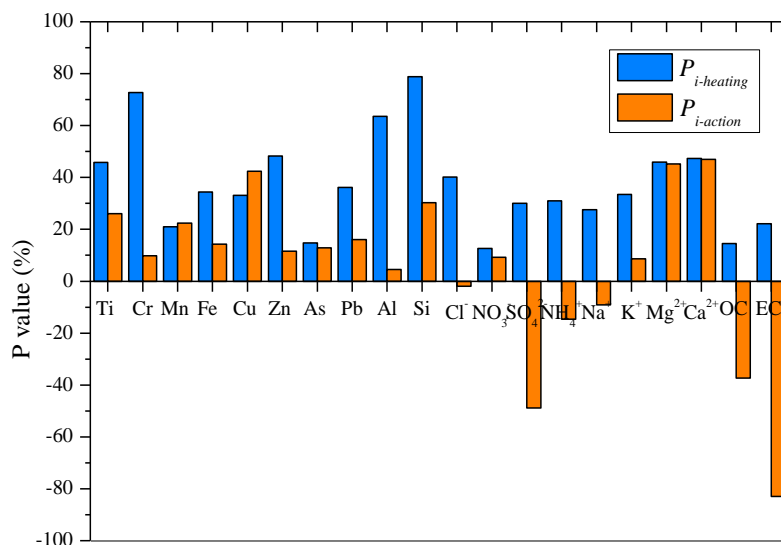


Fig. 8. The $P_{i\text{-heating}}$ and $P_{i\text{-action}}$ of chemical species in $\text{PM}_{2.5}$ during the TECA period in Shijiazhuang.

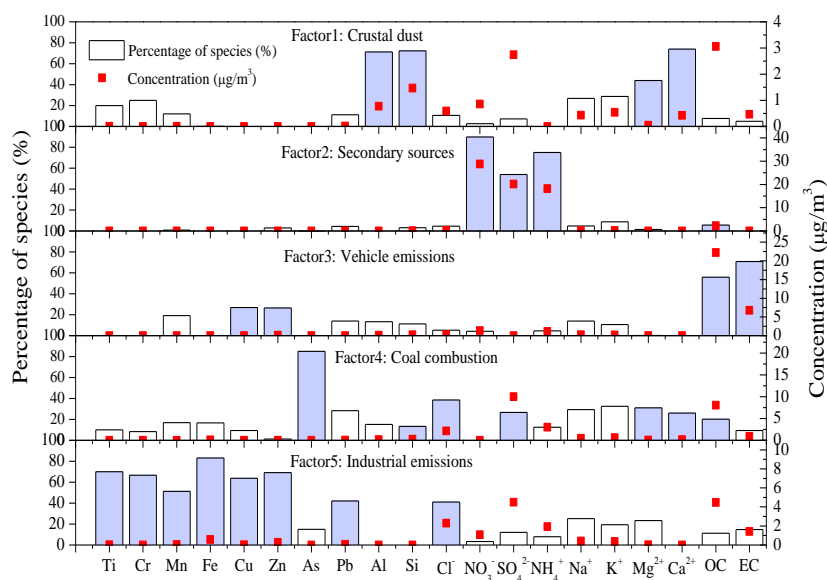


Fig. 9. Source profiles obtained with the PMF for $\text{PM}_{2.5}$. Filled bars identify the species that mainly characterize each factor profile.

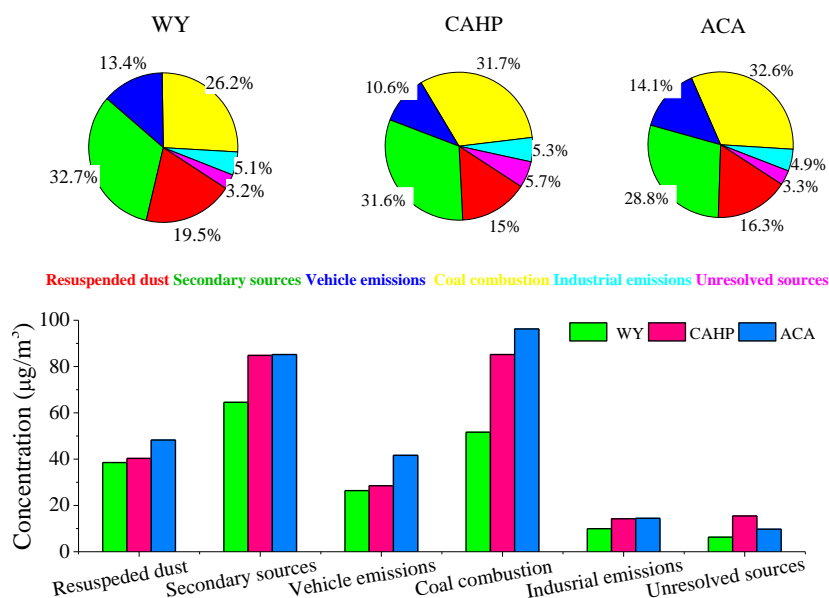


Fig. 10. Source contributions of PM_{2.5} during different stages in Shijiazhuang. WY represents whole year: November 24, 2015 to January 9, 2017.

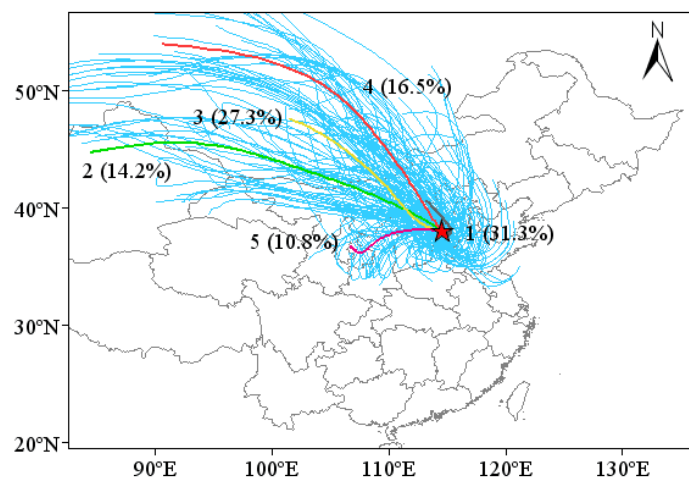


Fig. 11. Five clusters of the 72-h air mass backward trajectories during the CAHP. Red star represents Shijiazhuang city.

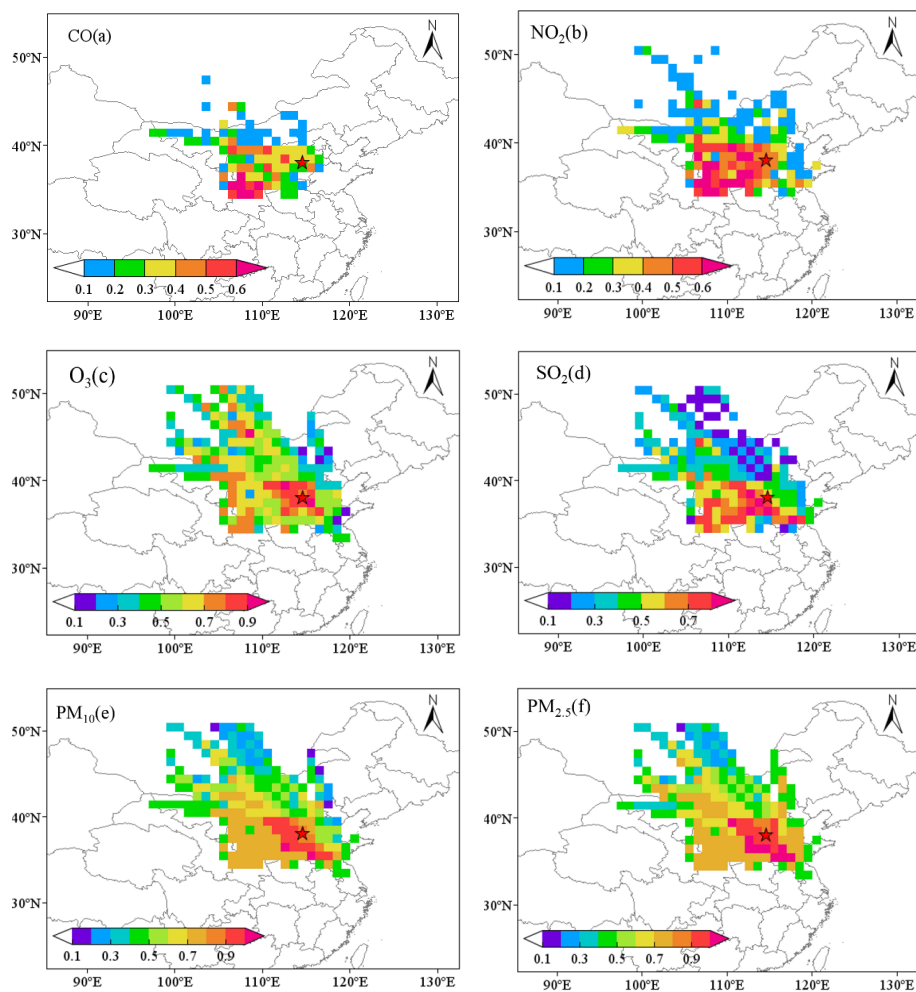


Fig. 12. Potential sources areas of atmospheric pollutants obtained from PSCF model during the CAHP. Red star represents Shijiazhuang city. The colors represent potential sources-areas influenced on the atmospheric pollutants, and the red color could be determined to be relatively important sources-areas while the blue color means unimportant potential sources-areas.



Table 1. The meteorological conditions during the four stages (NCANHP, NCAHP, CAHP and ACA) of the TECA period in Shijiazhuang.

	NCANHP		NCAHP		CAHP		ACA	
	Ave.	S.D.	Ave.	S.D.	Ave.	S.D.	Ave.	S.D.
Temperature (°C)	8.4	3.6	7.4	2.4	3.1	3.8	0.7	2.7
Relative humidity (%)	77.7	17.0	73.4	15.7	71.5	18.0	83.3	18.1
Wind speed (m/s)	0.7	1.2	0.6	0.6	0.4	1.0	0.5	1.1
Height of mixed layer (m)	540	144	590	274	474	299	431	360

Ave. represents average value, S.D. represents standard deviation. NCANHP represents the no control action and no heating period, NCAHP represents the no control action and heating period, CAHP represents the control action and heating period, and ACA represents after control action.

Table 2. The average concentrations of atmospheric pollutants in different clusters during the CAHP.

Clusters	Probability of occurrence (%)	Atmospheric Pollutants ($\mu\text{g}/\text{m}^3$)					
		SO ₂	NO ₂	O ₃	CO(mg/m ³)	PM ₁₀	PM _{2.5}
1	31.3	68	88	14	3.9	358	237
2	14.2	67	78	24	3.0	290	181
3	27.3	65	69	20	2.8	232	152
4	16.5	50	58	27	2.1	189	119
5	10.8	83	104	16	4.8	451	303